Composite Structures 110 (2014) 249–275

Contents lists available at ScienceDirect

Composite Structures

journal homepage: www.elsevier.com/locate/compstruct

Low-velocity impact responses of the stiffened composite laminated plates based on the progressive failure model and the layerwise/solid-elements method

D.H. Li, Y. Liu, X. Zhang *

School of Aerospace, Tsinghua University, Beijing 100084, China

ARTICLE INFO

Article history:
Available online 18 December 2013

Keywords:
Stiffened composite laminated plate
Low velocity impact
Progressive failure model
Layerwise/solid-elements method

ABSTRACT

Low-velocity impact responses and impact-induced damages evaluation problems are investigated for the stiffened composite laminated plates based on the progressive failure model and layerwise/solid-elements method (LW/SE). The LW/SE method, which was developed in our previous works (Li, Qing, et al., 2013; Li, Liu, et al., 2013) [1,2] for the composite laminated stiffened shells and sandwich plates, not only can obtain accurate displacements and stresses for composite laminates but also can consider complex stiffeners without any assumptions. In the present analysis method, impact responses are determined by the finite element code of LW/SE and the nonlinear Hertz's contact law which enables consideration of local indentation produced by the indentor on the impacted surface. The 3D Hashin criteria in quadratic strain is employed to predict the initiation of the impact-induced damages. The effect of the accumulation of the damages on the stiffness of laminated plate and stiffeners is computed by using continuum damage mechanics. Several numerical examples are carried out to demonstrate the excellent predictive capability of current method and to study the influence of parameters on the impact responses and impact-induced damages. In addition, the present analysis method is used to study the multi-impacts problem of the stiffened composite laminated plate.

1. Introduction

Composite materials are used in almost all aspects of the industrial and commercial manufacturing fields of aircrafts, ships, vehicles and other high performance structures due to their high specific stiffness and strength, excellent fatigue resistance, longer durability as compared to metallic structures, and ability to be tailored for specific applications. Particularly, in the field of aviation industry, its proportion in the structure has been considered as the one of most important indicators for the overall improvement of the aircraft. The behavior of composite laminated materials under low velocity impact is of concern in recent decades, since the damages induced by low velocity impact such as a dropped tool or debris from runways could reduce the strength of the structure significantly and furthermore the internal damages are not detectable through visible observation. If the impact-induced internal damages are not detected and repaired in time, the damage area will continuously grow and finally lead to complete structural collapse. Some comprehensive reviews can be found in Ref. [3,4] for the literatures focused on low velocity impact on composite materials.

According to Abrate [5], the analysis models used to obtain the impact response can be classified into three categories: energy-balance models, spring-mass models and complete models. In the energy-balance models, the impact dynamic is to consider the balance of energy in the system and the structure behaviors are quasi-statical. When the structure reaches its maximum deflection, the velocity of the impactor becomes zero and all the initial kinetic energy has been used to deform the structure. In most complete spring-mass models, the linear stiffness of the structure, the nonlinear membrane stiffness and the contact force are represented by the spring models, the effective mass of the structure and the impactor are represented by the mass models. Therefore, the impact dynamic system can be simplified to a two-degree-of-freedom model or one-degree-of-freedom model. The stiffness used in the spring-mass models can be determined from theoretical formulas available in many handbooks, or numerically using the finite element method. With a complete model, the dynamic behavior of the structure is described accurately. Usually, in many cases the classical plate theory can be used but, in some cases, transverse shear deformations become significant and higher-order theories must be used. For the plate behaving in a quasi-static manner,

* Corresponding author. Tel.: +86 1062782078.
E-mail addresses: lidinghe@163.com (D.H. Li), yan-liu@tsinghua.edu.cn (Y. Liu), xzhang@tsinghua.edu.cn (X. Zhang).

0263-8223/$ - see front matter © 2013 Elsevier Ltd. All rights reserved.
http://dx.doi.org/10.1016/j.compstruct.2013.12.011

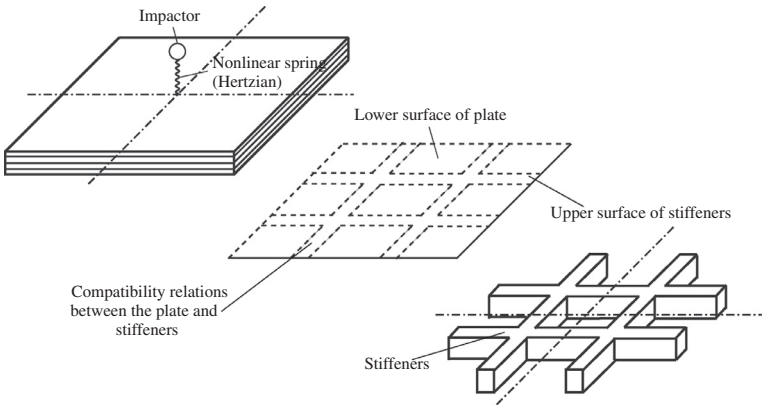

Fig. 1. A composite laminated plate or cylindrical shell with stiffeners impacted by a steel sphere.

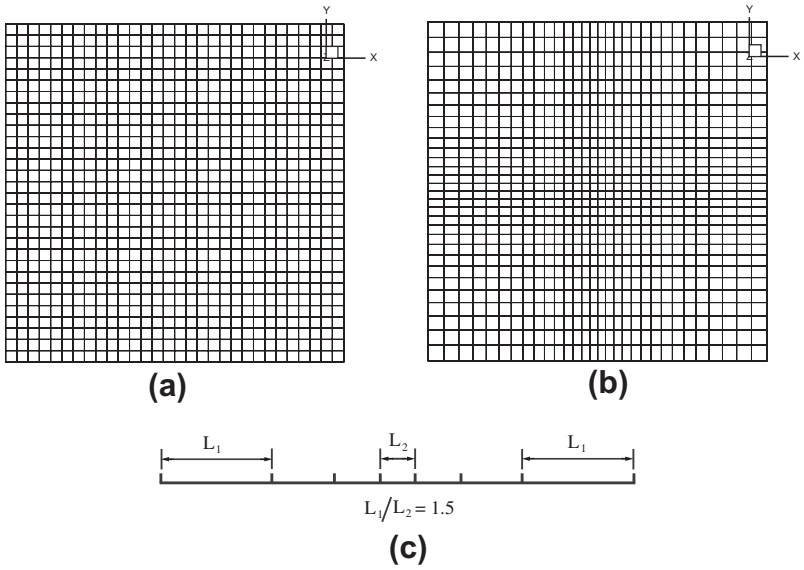

Fig. 2. Finite element discretization. (a) Uniform finite elements; (b) nonuniform finite elements; and (c) type "Two way bias" used in nonuniform finite elements.

the bending waves induced by impact travel from the contact point to the boundary of the plate and back many times during the predicted contact duration, the boundary controlled impact and the spring mass model or an energy balance approach might be adequate. If the deformation never reaches the edges of the plate during the predicted contact duration, very good results can be provided by the wave-controlled impact and the approximate solution. For the intermediate cases, reflected waves will affect the contact force history significantly, so a complete model taking into account the full dynamic behavior of the plate and the boundary conditions is necessary.

Without considering the impact-induced damage, there are a number of research works focusing on the responses analysis problem of low velocity impact for the composite laminated shells/plates. Sun [6] and Dobyns [7] used the analytical method of plate developed by Whitney and Pagano [8] to analyze a simply supported orthotropic plate subjected to a central impact. Sun and Chen [9] investigated the impact response behaviors of the initially stressed composite laminates by using finite element method and Newmark integration algorithm. Cairns and Lagace [10] studied the influence of different parameters on the impact behaviors of laminated composite plates by using Rayleigh–Ritz method to spatially discretize the time-varying boundary value problem and using Newmark integration algorithm method to integrate the motion equations. The effects of shearing deformation, bending-twisting coupling, and nonlinear contact behavior were considered. Wu and Chang [11] carried out a transient dynamic finite element analysis for the responses of the composite laminated plates subjected to transverse foreign object impact. An 8-point brick element with incompatible modes was developed in this analysis, and the direct Gauss quadrature integration scheme was used through the element thickness to account for the change in material properties from layer to layer within the element. The Newmark scheme was adopted to perform time integration from step to step, and a contact law incorporated with the Newton–Raphson method was applied to calculate the contact force during impact. Gong et al. [12] developed a spring-mass model to determine the contact force between the shell and impactor during impact. In this model, the contact force was described by an analytic function in terms of the material properties and mass of the shell and impactor, as well as the impact velocity. And then, based on a higher-order shear deformation theory (HSDT), Gong et al. [13] presented a set of analytical solutions to predict the dynamic response of the simply-supported, doubly curved, cross-ply laminated shells impacted by a solid striker. Nosier et al. [14] used a layerwise theory and model superposition technique to investigate the low velocity

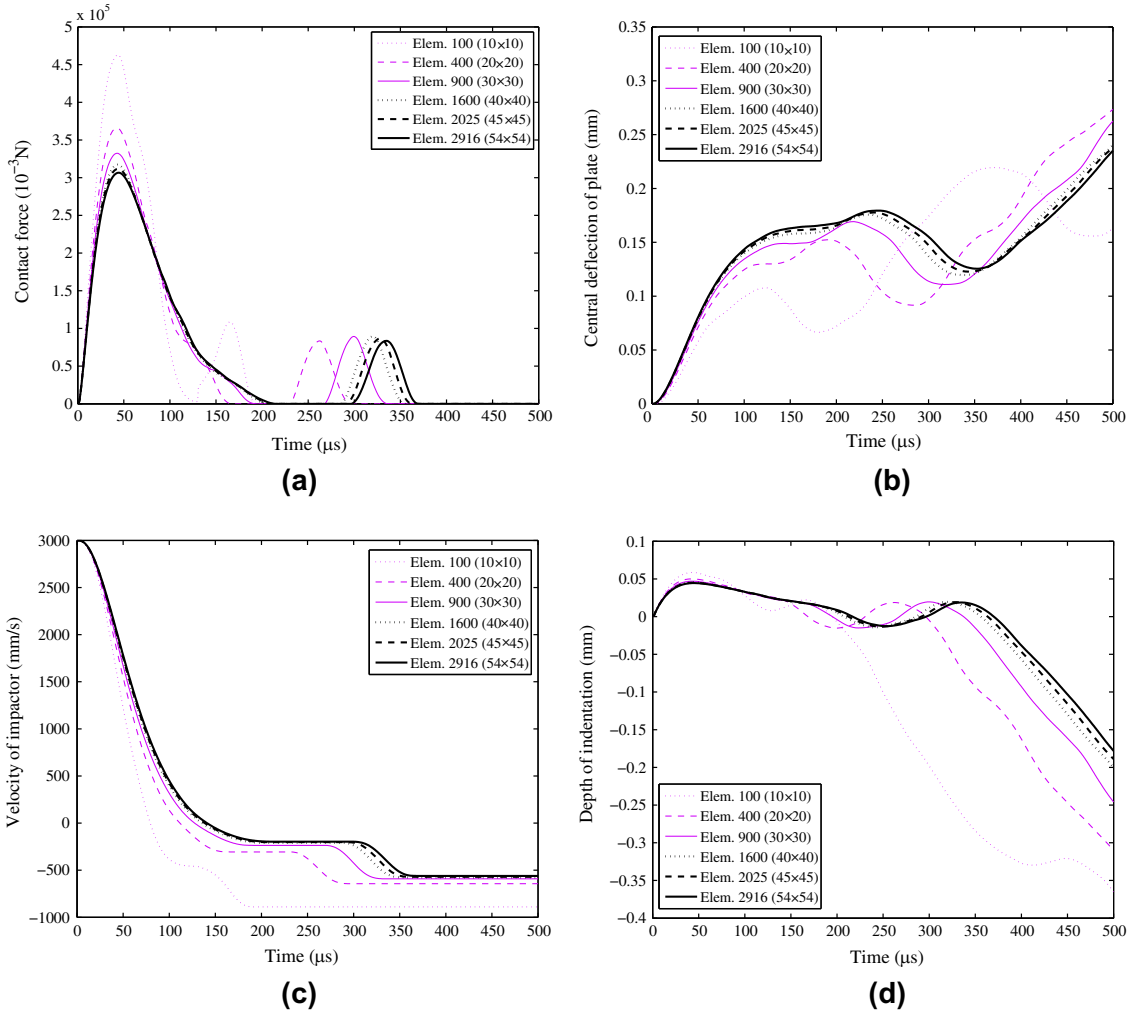

Fig. 3. Convergence test. (a) Contact force; (b) displacement w at the contact point ($x = y = a/2$, $z = h/2$), (c) velocity of the impactor and (d) indentation depth.

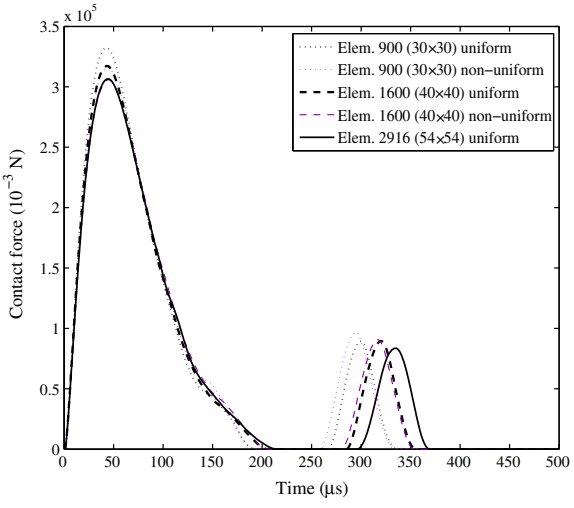

Fig. 4. Effect of the finite element scheme on the contact force.

impact response of composite laminated plates, and the contact area is time dependent. Chandrashekhara and Schroeder [15] developed a finite element model for the nonlinear impact response of composite laminated cylindrical and doubly curved shells based on Sander's shell theory and the modified Hertzian contact law. Using a linearized contact law, Choi and Lim [16] studied low-velocity impact analysis of composite laminates, it could be shown that the linearized contact law could be well applied to the low-velocity impact analysis of composite laminates.

In all above works the impact-induced damages predicition was not considered. Choi and Chang [17,18] performed an investigation consisting of both analysis and experiments to fundamentally understand the failure mechanisms and mechanics of fiber-reinforced composites resulting from impact and to identify the essential parameters governing the impact damage. And then, Choi and Chang [19] presented a model for predicting the initiation of the damages and the extent of the final damages as a function of material properties, laminate configuration and impactor's mass. The impact damages in terms of matrix cracking and delaminations resulting from a point-nose impactor were the primary concern. Kim et al. [20] investigated the dynamic behavior and impact-induced damage of the composite laminated curved structures by using the incompatible eight-noded brick elements with Taylor's modification and a modified Hertzian contact law. Krishnamurthy et al. [21,22] determined the impact responses of a composite laminated cylindrical shell by a nonlinear Hertzs contact law. The impact-induced damage was evaluated by the semi-empirical damage prediction model of Choi-Chang [17,18]. The effects of important parameters, such as impactor mass and

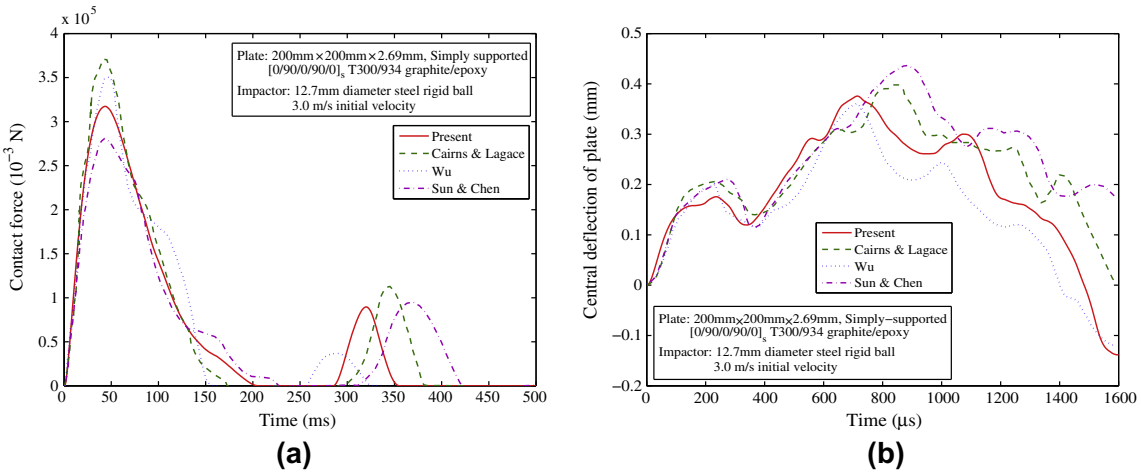

Fig. 5. Comparison of the impact responses with the results obtained by other authors. (a) Contact force history; and (b) central deflection at the neutral surface.

Table 1
Material properties of the composite laminates.

Elastic properties (GPa)	E_{11}	E_{22}	E_{33}	G_{12}	G_{13}	G_{23}
	156.5	13.0	13.0	6.96	6.96	3.45
	v_{12}	v_{13}	v_{23}			
	0.23	0.23	0.4			
Strength properties (MPa)	$\sigma_{11}^{f,t}$	$\sigma_{11}^{f,c}$	$\sigma_{22}^{f,t}$	$\sigma_{22}^{f,c}$		
	1516.8	1592.7	44.5	253.0		
	σ_{12}^{f}	σ_{13}^{f}	σ_{23}^{f}			
	106.9	106.9	106.9			
Fracture energy (N/mm)	$G_{t,1}$	$G_{c,1}$	$G_{t,2}$	$G_{c,2}$	$G_{t,3}$	$G_{c,3}$
	20	20	0.23	0.76	0.23	0.76

velocity, shell curvature and stacking sequence of plies, are investigated as well.

In contrast to the number of studies dealing with impact on the composite plates and shells, few papers focus on the topic of impact on stiffened composite plates and shells. Since stiffened composite plates are commonly utilized in a variety of engineering structures, an understanding of the various effects of stiffeners on the impact response is important to assess the strength and reliability of the structures. Gong and Lam [23] presented an approximate solution to predict the transient response of stiffened composite plates impacted by a solid striker. In this approximate solution, the stiffened composite plate is characterized by a fictitious orthotropic layer whose bending and extensional properties are those of the individual stiffeners averaged out over representative areas. Seydel and Chang [24,25] developed a real-time identification technique for the contact force history of low-velocity impacts on the composite panels with beam stiffeners by both analysis and experiments. Faggiani and Falzon [26] presented an intralaminar damage model for the damage mechanisms occurring in carbon fiber composite structures incorporating fiber tensile and compressive breakage, matrix tensile and compressive fracture, and shear failure on the basis of a continuum damage mechanics approach. The aim of the present work is to estiblish a method for low velocity impact responses and impact-induced damages prediction of the stiffened composite laminated plates. Furthermore, the developed method can be used to obtain the low-impact responses and impact-induced damages of the composite laminated plate stiffened with complex stiffeners without any assumption and simplification.

The widespread application of the stiffened plates/shells has resulted in different methods of performing appropriate structural analysis. A large number of studies on bending, buckling, and vibration are available in the literature. During last 20 years, a lot of analysis schemes have been developed such as the methodology based on energy principles [27,28], the semi-analytical methods [29,30], the differential quadrature methods [31], the finite element methods (FEM) [32–34,1,35–42], the meshfree methods [43–47], and the boundary element methods (BEM) [48,49] or a combination of finite element methods and boundary element methods [50]. Among these approaches, the finite element method is the most widely used numerical method for the stiffened composite plates/shells. There are two main schemes to deal with the relationship between the plate and stiffeners in aforementioned methods: the one is that the closely spaced stiffeners are averaged out or "smeared over" the shell surface, and anther is that the stiffeners are equivalent as beams. These approximation may be applicable only if the ratios of spacing between two consecutive stiffeners to plate dimensions are small enough to ensure approximate homogeneity of stiffness, and the ratio of stiffener rigidity to the plate rigidity must not become so large that the beam action is predominant. So several assumptions must be made in order to facilitate a solution if the stiffeners are not identical or unequally spaced.

Moreover, stiffened composite structures have been widespread in recent years due to the economic and structural advantages of such systems. The complication would further increase when analyzing stiffened composite laminated plate/shell structures. Therefore, it is very necessary to develop an analysis method which not only can obtain the accurate displacements and stresses of composite laminated plates/shells but also can consider the complex stiffeners without any assumption and simplification. In the earlier studies of the present authors [1,2], a layerwise/solid-element (LW/SE) method was established based on the layerwise theory and the solid elements for the composite stiffened laminated cylindrical shells. In LW/SE method, the layerwise theory was used to model the behavior of the composite laminated cylindrical shells, and the eight-noded solid element is employed to discrete the stiffeners without any assumption and simplification. The displacements freedoms of layerwise theory in the surface of plates/shells appear in the governing equations, and the freedom of the in-plane nodes of the layerwise theory is equal to that of the brick element. It means that the governing equations of the plates and shells established based on the layerwise theory can be simultaneously solved with the governing equations of stiffeners discreted by the solid elements and therefore enables to ensure the compatibility of displacements at the interface between shells and stiffeners through the compatibility conditions.

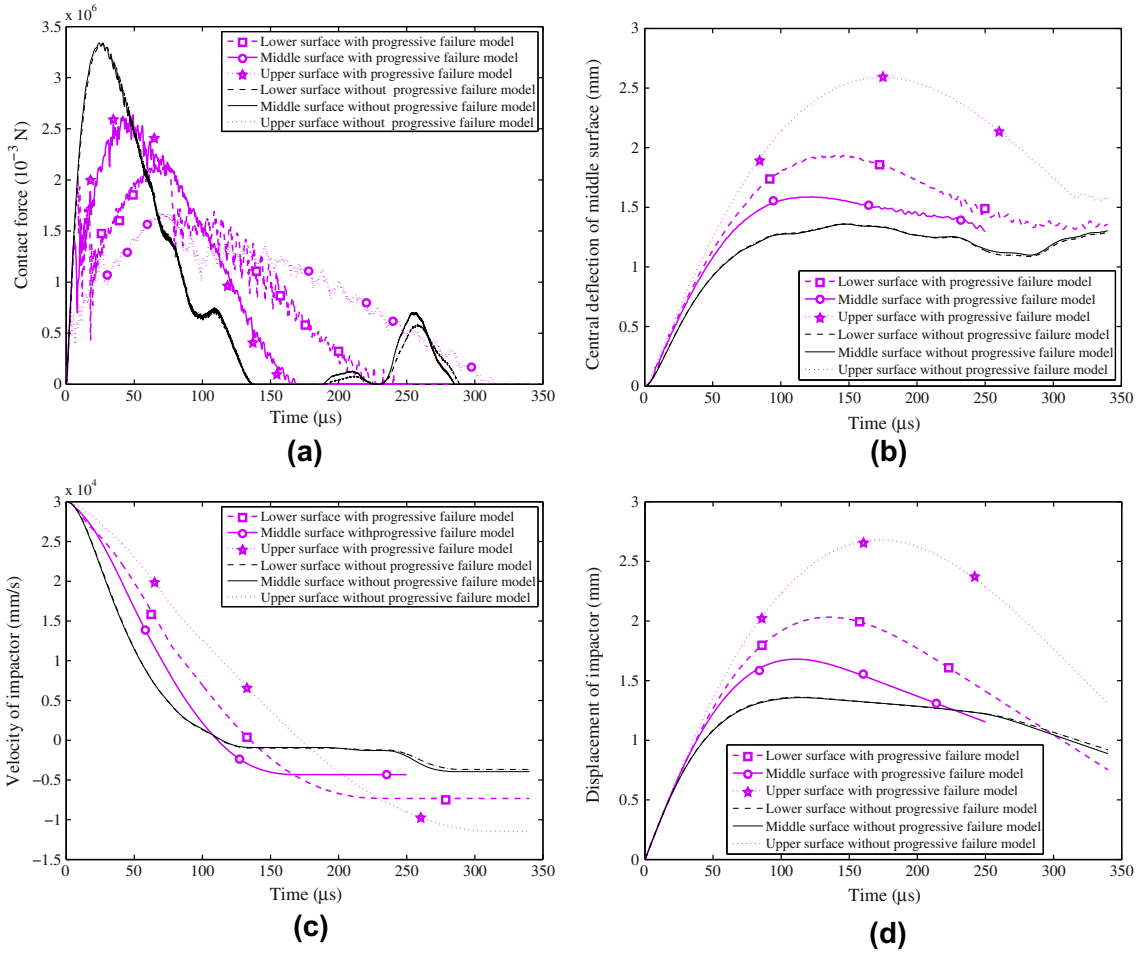

Fig. 6. The impact responses of composite laminated plate with/without the progressive damage analysis model. (a) Contact force; (b) central deflection of plate at middle surface, (c) velocity of impactor; and (d) displacement of the impactor.

It is well known that damage in composite material is generally complicated consisting of multiple failure modes such as fiber breakage, fiber pullout, matrix cracking, fiber–matrix debonding, delamination between plies, etc. Methods for modeling material damage of composite materials can be divided into micromechanics of damage and continuum damage mechanics approaches (CDM) [51]. Micromechanics has been developed and applied in composite failure mechanism related to the damage of either the fibers or the matrix separately. It is valuable tools to gain insights into mechanisms and failure processes at the micro-scale. It also can be used in the global response of the composite structures. However, a significant limitations with the micromechanics models is the large number of material parameters need to identify the constitutive model and the high computational cost. Since composite structures can accumulate damage before structural collapse, the use of failure criteria is not sufficient to predict ultimate structural failure. To bridge this gap, the progressive failure has been developed and enhanced for composite materials. Simplified models, such as the ply discount method, can be used to predict ultimate failure, but cannot represent with satisfactory accuracy the quasi-brittle failure characteristic of a laminate that results from the accumulation of different damage mechanisms. In order to conjugate simplicity of application and accuracy of results, the concept of distributed damage and the use of formulations based on the thermodynamics of continuum media play a fundamental role. In this framework, CDM considers damaged materials as a continuum, in spite of heterogeneity, micro-cavities, and micro-defects.

In the present work, the LW/SE method, modified nonlinear Hertz's law and progressive failure model are employed to develop a method for low impact responses and impact-induced damage prediction of the stiffened composite laminated plates. Firstly, the transient response analysis model of the stiffened composite laminated plate is estiblished by using the LW/SE method and Newmark method, the contact force between the stiffened plate and impactor is obtained by the modified nonlinear Hertz's law with Newmark method and Newton–Raphson iterative method, and the prediction of impact-induced damages is carried out by the 3D Hashin criteria and progressive failure model. And then, numerical examples are carried out to demonstrate the excellent predictive capability of current method and to study the effect of the load application point of equivalent contact force in thickness direction on the impact responses. For two kinds of stiffened composite laminated plates, the influence of important parameters on the impact responses and impact-induced damages is investigated as well, such as the impact velocity, radius of impactor and thickness of stiffeners. At last, the present analysis method is used to study the multi-impacts problem of stiffened composite laminated plate.

2. Contact force of low-speed impact based on Hertz's law

Krishnamurthy and Mahajan [22,21] developed a nonlinear Hertz's law for the low-impact problem of the composite laminated cylindrical shell. A brief theoretical deviration of the modified nonlinear Hertz's contact low for the plates and the

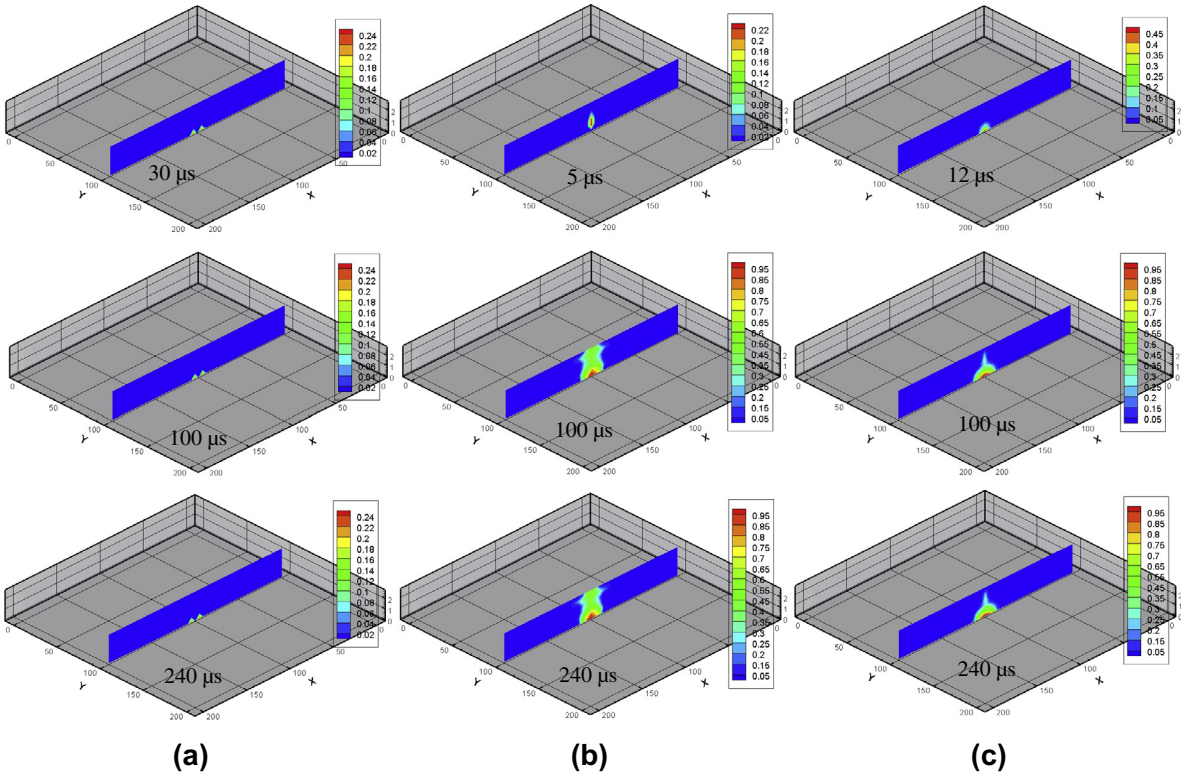

Fig. 7. The damage variations of the composite laminated plate subjected to impact load at the lower surface. (a) Damage variation d_1 (fiber breakage); (b) damage variation d_2 (matrix cracking); and (c) damage variation d_3 (delamination).

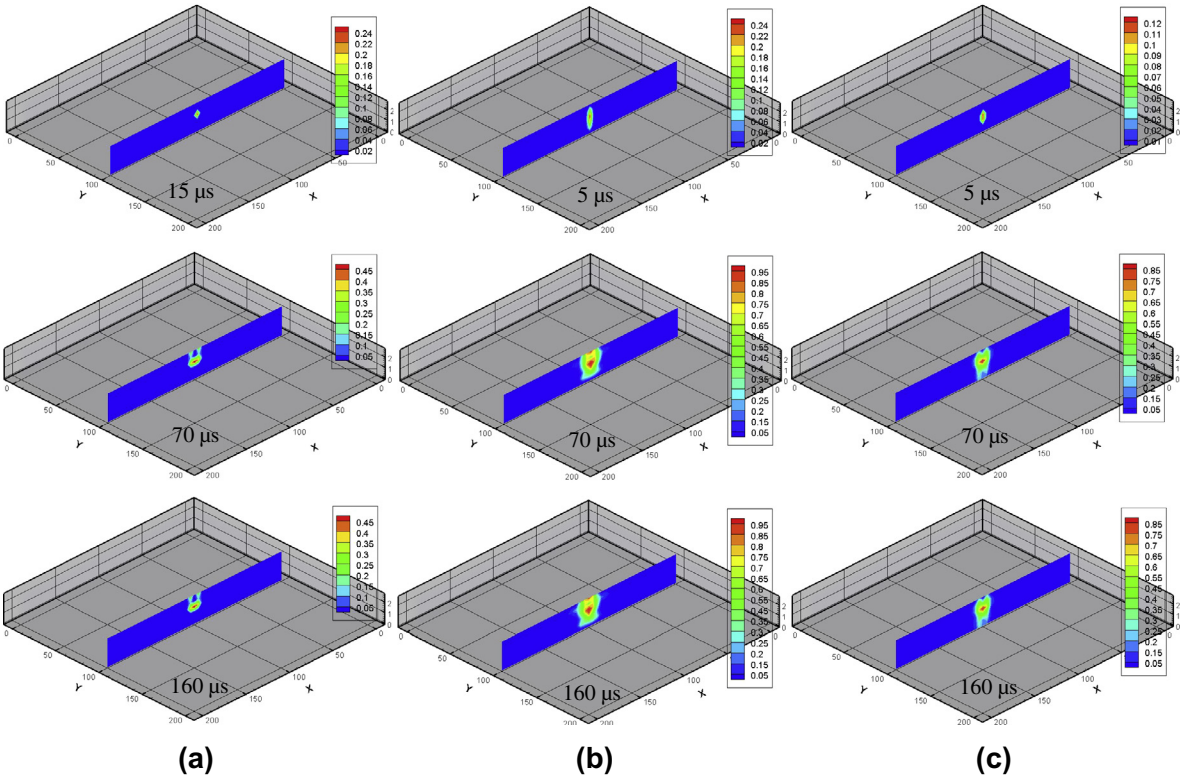

Fig. 8. The damage variations of the composite laminated plate subjected to impact load at the middle surface. (a) Damage variation d_1 (fiber breakage); (b) damage variation d_2 (matrix cracking); and (c) damage variation d_3 (delamination).

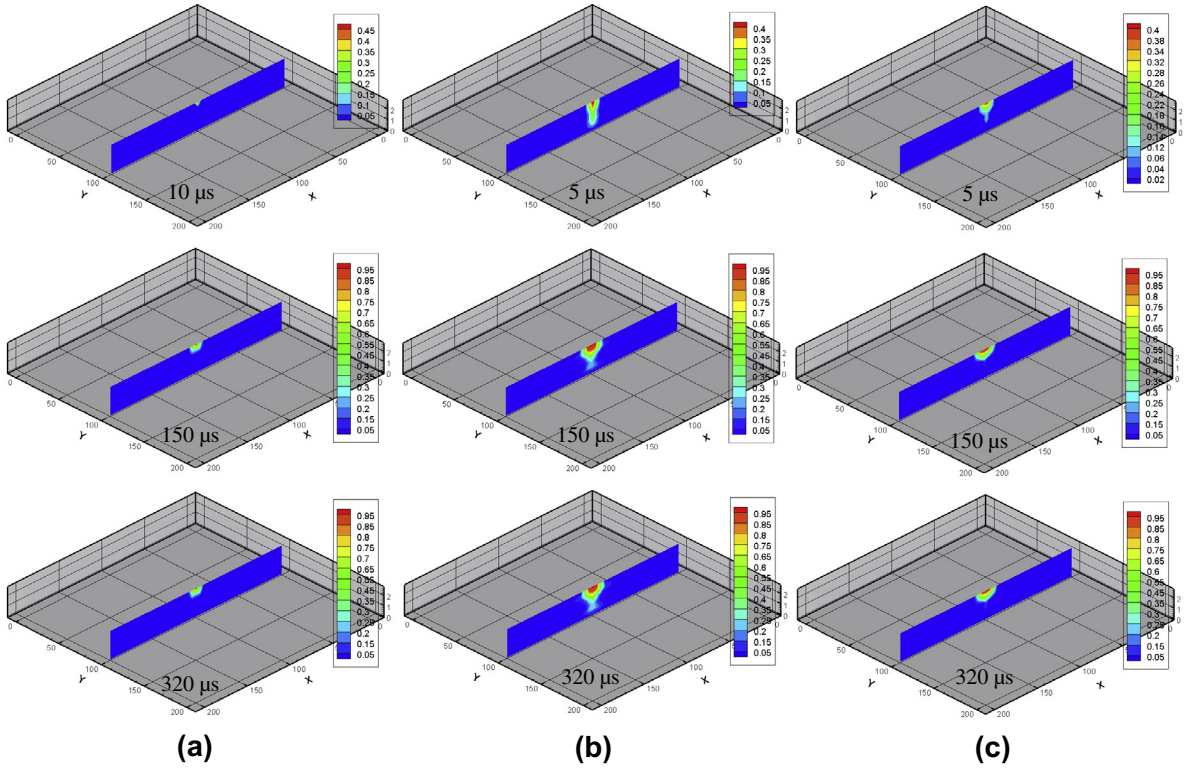

Fig. 9. The damage variations of the composite laminated plate subjected to impact load at the upper surface. (a) Damage variation d_1 (fiber breakage); (b) damage variation d_2 (matrix cracking); and (c) damage variation d_3 (delamination).

Table 2
Initial time points of the fiber breakage, the matrix cracking and the delaminations.

Load position in thickness direction	Damage form (μs)		
	Fiber breakage	Matrix cracking	Delaminations
Lower surface	21	3	9
Middle surface	13	4	5
Upper surface	7	2	3

cylindrical shells is presented in this section together with the reloading phase. According to Newton's second law the equation of motion for a rigid impactor is given by

$$m_i \ddot{w}_i = -f_c \tag{1}$$

where m_i and $\ddot{w}_i$ are the mass and the acceleration of the impactor, respectively. f_c is the contact force between impactor and target body.

Three kinds of phases (loading, unloading and reloading phase) probably occur during the impact. By using the Hertzian contact theory, the contact force f_c can be related to the indentation depth as follow [52]

$$f_c = \begin{cases} k\alpha^{1.5} & \text{loading} \\ f_m\left(\frac{\alpha-\alpha_0}{\alpha_m-\alpha_0}\right)^{2.5} & \text{unloading} \\ f_m\left(\frac{\alpha-\alpha_0}{\alpha_m-\alpha_0}\right)^{1.5} & \text{reloading} \end{cases} \tag{2}$$

where $\alpha(t) = w_i(t) - w_t(t)$ is the depth of indentation, $w_t(t)$ is the displacement of composite laminated plate at the contact point, f_m and α_m are the maximum contact force and indentation at the beginning of unloading, k is the modified constant of the Hertz's contact theory which is given by

$$k = \begin{cases} \frac{4}{3}\left(\frac{1}{r_i}+\frac{1}{2R_c}\right)^{-0.5} \Big/ \left[\frac{(1-\nu_i)^2}{E_i}+\frac{1}{E_2}\right] & \text{cylindrical shell} \\ \frac{4}{3}\sqrt{r_i}\Big/\left(\frac{1-\nu_i^2}{E_i}+\frac{1}{E_2}\right) & \text{plate} \end{cases} \tag{3}$$

where r_i and R_c are the radius of the impactor and the cylindrical shell, respectively; E_i and E_2 are the Young's modulus of the impactor and the elastic modulus transverse to the fiber direction, respectively; ν_i is the Poisson's ratio of the impactor.

α_0 in Eq. (2) denotes the permanent indentation in a loding-unloading cycle which is given by

$$\alpha_0 = \begin{cases} 0 & \alpha_m < \alpha_{cr} \\ \alpha_m\left[1-\left(\frac{\alpha_{cr}}{\alpha_m}\right)^{2/5}\right] & \alpha_m \geqslant \alpha_{cr} \end{cases} \tag{4}$$

where α_{cr} is the critical indentation, and it has been taken to be 8.03×10^{-2} mm for graphite/epoxy composite laminates and 1.016×10^{-1} mm for glass/epoxy composite laminates.

The displacement and velocity of impactor at time step $n+1$ can be detemined by Newmark's integration scheme, as

$$w_i^{n+1} = w_i^n + \dot{w}_i^n \Delta t + \ddot{w}_i^n\left(\frac{\Delta t^2}{4}\right) - f_c^{n+1}\left(\frac{\Delta t^2}{4m_i}\right) \tag{5}$$

Substituting Eq. (5) into the modified contact laws defined in Eq. (2), one obtains the implicit expressions between the displacement of target body w_t and the contact force at time step $n+1$ as

$$f_c^{n+1} = \begin{cases} k\left[w_i^* - w_t^{n+1} - \left(\frac{\Delta t^2}{4m_i}\right)f_c^{n+1}\right]^{1.5} & \text{loading} \\ \frac{f_m}{(\alpha_m-\alpha_0)^{2.5}}\left[w_i^* - w_t^{n+1} - \alpha_0 - \left(\frac{\Delta t^2}{4m_i}\right)f_c^{n+1}\right]^{2.5} & \text{unloading} \\ \frac{f_m}{(\alpha_m-\alpha_0)^{1.5}}\left[w_i^* - w_t^{n+1} - \alpha_0 - \left(\frac{\Delta t^2}{4m_i}\right)f_c^{n+1}\right]^{1.5} & \text{reloading} \end{cases} \tag{6}$$

where $w_i^* = w_i^n + \dot{w}_i^n \Delta t + \ddot{w}_i^n\left(\frac{\Delta t^2}{4}\right)$.

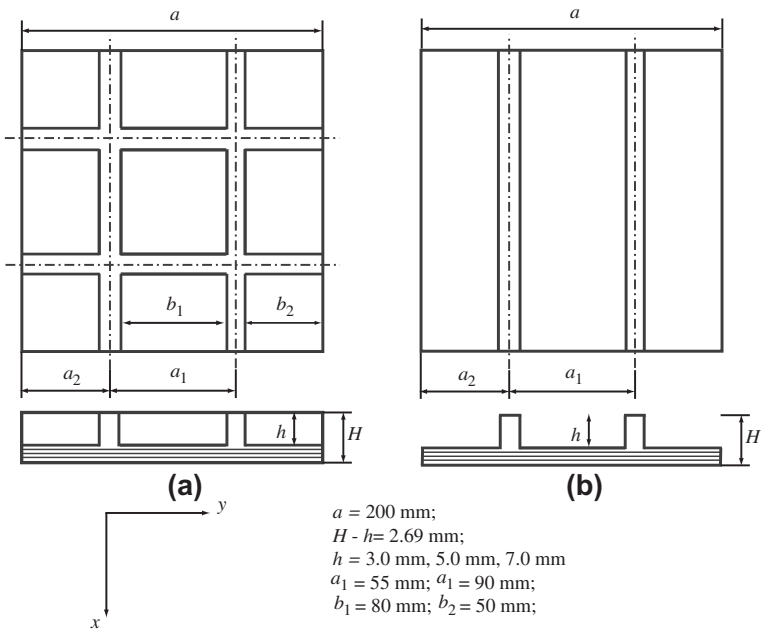

Fig. 10. Two kinds of stiffened composite laminated plates. (a) Concentrically stiffened laminated plates with four stiffeners; and (b) parallelly stiffened laminated plates with two stiffeners.

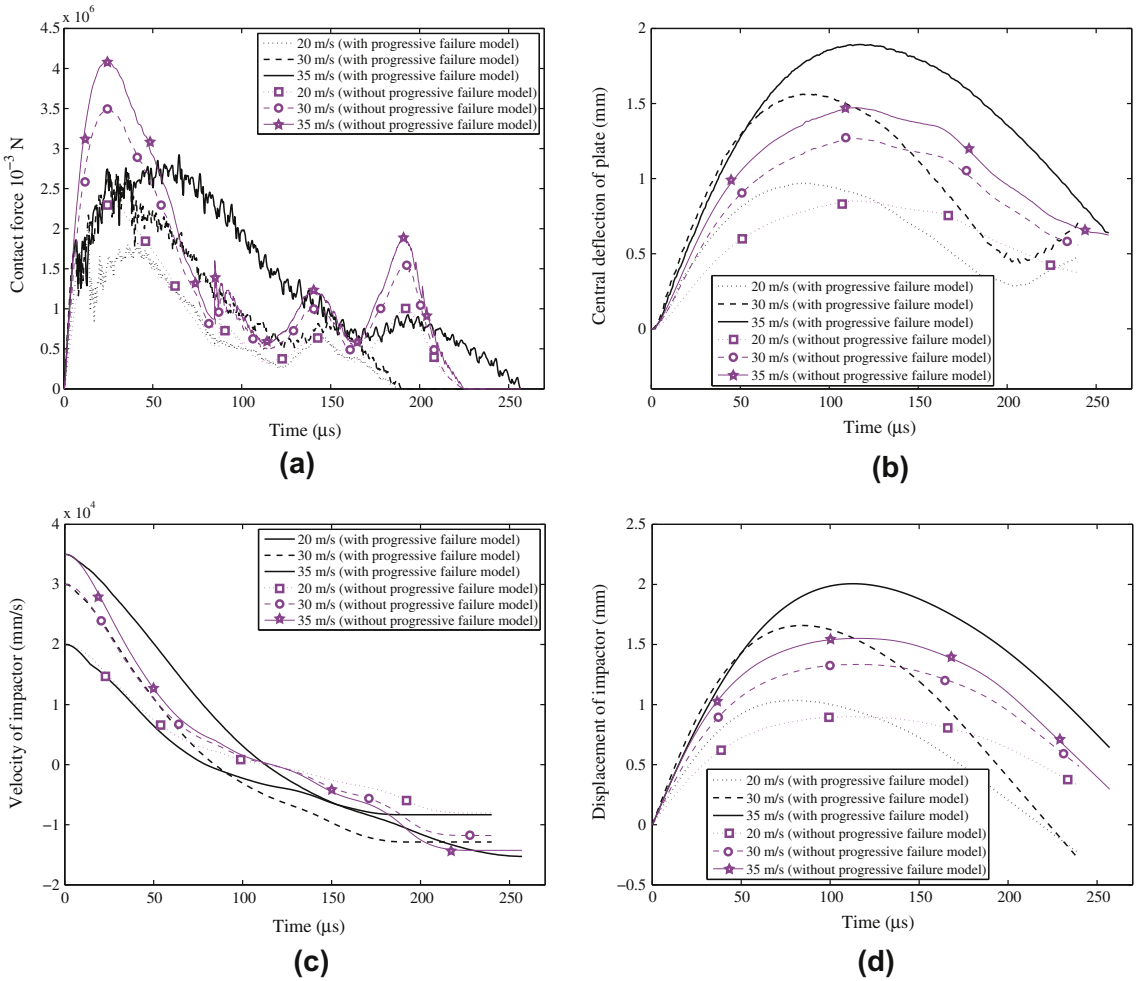

Fig. 11. Influences of the impact velocity on the impact responses of concentrically stiffened composite laminated plates with/without the progressive damage analysis model. (a) Contact force; (b) displacement *w* of plates in contact point, (c) velocity of the impactor and (d) displacement of the impactor.

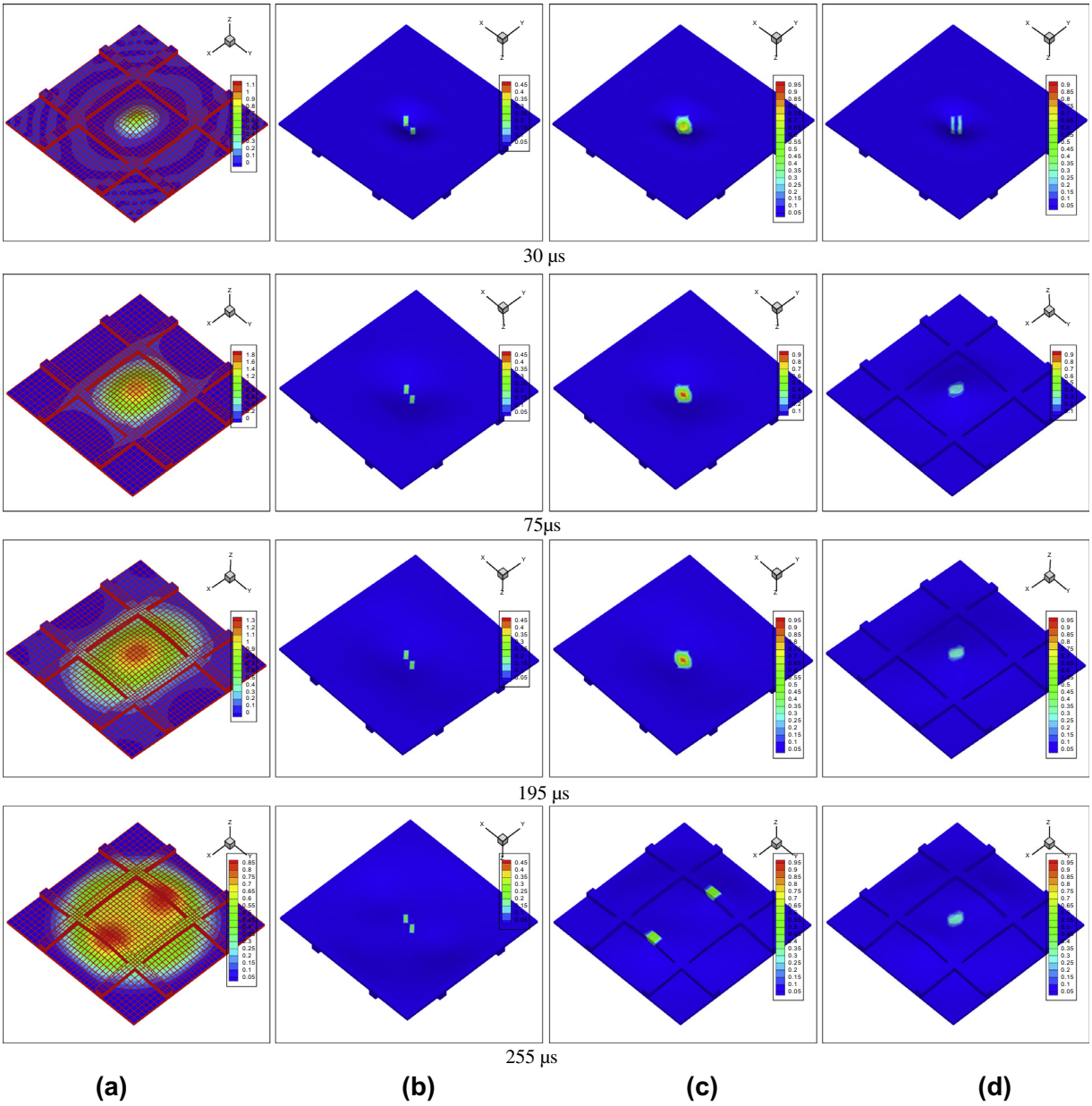

Fig. 12. The deformation and the damage histories of concentrically stiffened composite laminated plates subjected to impact velocity 30 m/s. (a) Deformation and nephogram of displacement w; (b) damage variation d_1 (fiber breakage); (c) damage variation d_2 (matrix cracking); and (d) damage variation d_3 (delamination).

3. Mathematic model of the composite laminated stiffened plates/shells subjected to impact

3.1. Layerwise theory of composite laminated plates/shells

In contrast to the equivalent single layer theory [53–56], the layerwise theories [57–62] are developed by assuming that the displacement field exhibits only C0-continuity through the laminate thickness. Thus the displacement components are continuous through the laminate thickness but the derivatives of the displacements with respect to the thickness coordinate may be discontinuous at various points through the thickness, thereby allowing for the possibility of continuous transverse stresses at interfaces separating dissimilar materials.

The Layerwise Shell Theory (LWST) of Reddy [59] gives an accurate description for the displacement field in the thickness direction. The three-dimensional displacement field is expanded as a function of a surface-wise two dimensional displacement field and a one-dimensional interpolation function through the thickness. The use of higher order polynomial interpolation functions or more sub-divisions through the thickness improves the accuracy of the displacement field. In the layerwise laminate theory, the displacements at point (x,y,z) in the composite laminated plates are assumed to be as

$$\begin{aligned} u(x,y,z) &= \sum_{i=1}^{N+1} u_i(x,y)\phi_i(z), \\ v(x,y,z) &= \sum_{i=1}^{N+1} v_i(x,y)\phi_i(z), \\ w(x,y,z) &= \sum_{i=1}^{N+1} w_i(x,y)\phi_i(z), \end{aligned} \tag{7}$$

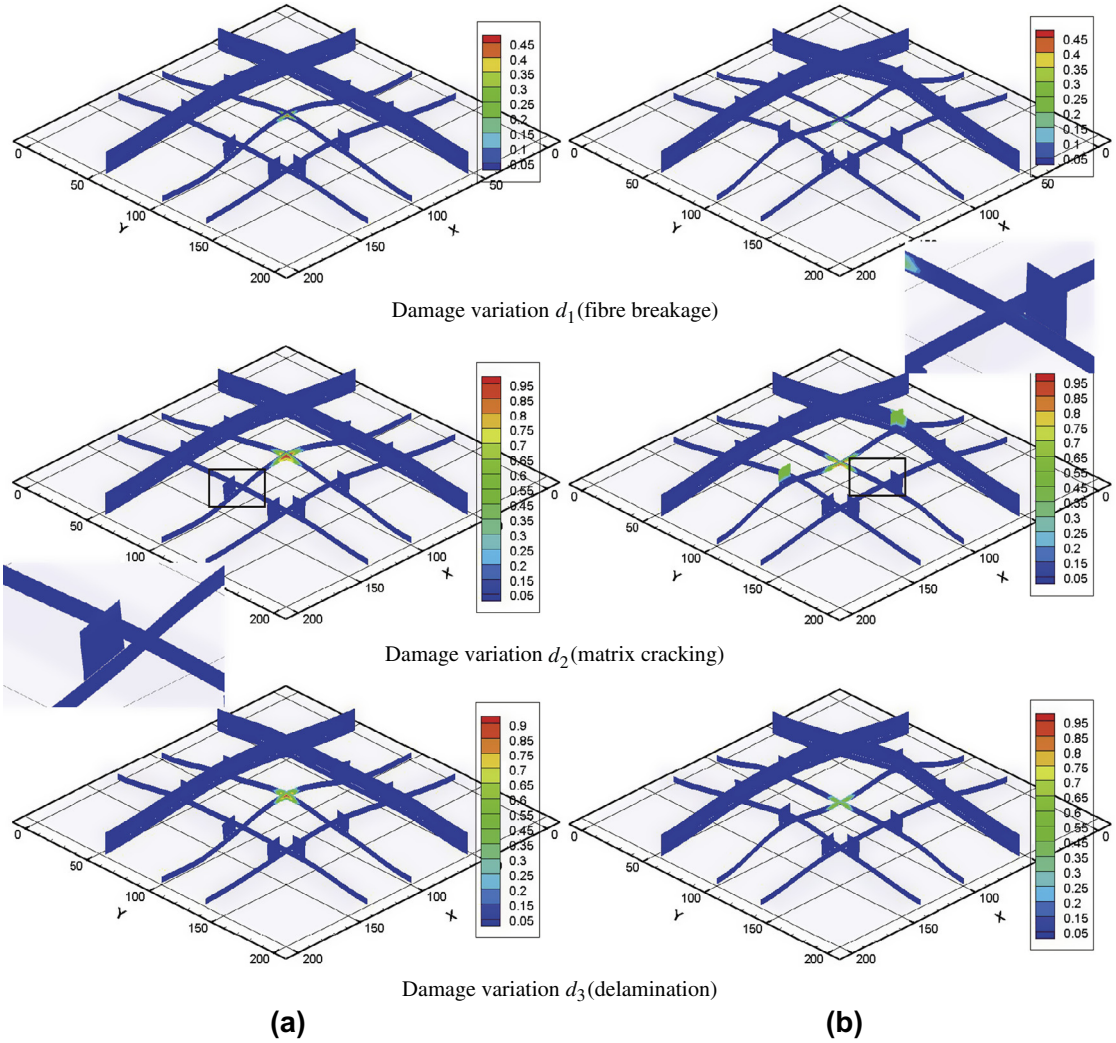

Fig. 13. Influence of impact velocity on damage variations distributions of concentrically stiffened composite laminated plates with four stiffeners, where the radius of impactor 6.0 mm and the thickness of stiffeners is 7.0 mm. (a) Impact velocity 30 m/s; and (b) impact velocity 35 m/s.

where u, v and w represent the displacement components of point $P(x,y,z)$ in the x, y and z directions, respectively. ϕ_i is a 1D linear Lagrangian interpolation function through the thickness of the laminated plate. The laminate thickness dimension is subdivided into a series of N one-dimensional finite elements ($Ne = N+1$ nodes) whose nodes are located in planes parallel to xy plane in the undeformed laminated facesheets. u_i, v_i and w_i are the nodal values of the 1D linear Lagrangian interpolation function through the thickness direction. N is also the number of mathematical layers of the laminated plates, which may be equal or less than the number of physical layers.

In order to develop the finite element formulation, the nodal displacement functions u_i, v_i and w_i are approximated on the ith plane of the plate by

$$\begin{aligned} u_i(x,y) &= \sum_{n=1}^{n_{elm}} u_i^n \psi^n(x,y), \\ v_i(x,y) &= \sum_{n=1}^{n_{elm}} v_i^n \psi^n(x,y), \\ w_i(x,y) &= \sum_{n=1}^{n_{elm}} w_i^n \psi^n(x,y), \end{aligned} \tag{8}$$

where n_{elm} is the number of nodes in each 2D element, $\varphi(x,y)$ is standard 2D finite element shape function, u_i^n, v_i^n and w_i^n are the displacement components of nth node of the 2D finite element representing the ith plane of the physical laminates element.

The finite element formulation of the present layerwise theory can be derived using the principle of virtual displacements in matrix form as

$$\boldsymbol{M}\ddot{\boldsymbol{U}} + \boldsymbol{K}\boldsymbol{U} = \boldsymbol{F} \tag{9}$$

Since the contact area is so small in comparison with the dimensions of the plate, the contact pressure between the impactor and plates can be considered as a concentrated (point) load at the central of plates/shells for the low-impact response analysis based on Hertz's law. Therefore, except the nodel component of the contact point in the direction of impact, all the components of load vector $\boldsymbol{F}$ in Eq. (9) are zero. The load vector $\boldsymbol{F}$ can be rewritten as

$$\boldsymbol{F} = \{0, 0, \ldots, f_c, \ldots, 0, 0\}^{\mathrm{T}} \tag{10}$$

3.2. Layerwise/solid-elements method of the composite laminated stiffened plates/shells

A layerwise/solid-element method has been developed in our previous work [1] for the linear static and free vibration analysis of composite stiffened laminated cylindrical shell. Only the essential details are provided in this section, see Ref. [1] for more details.

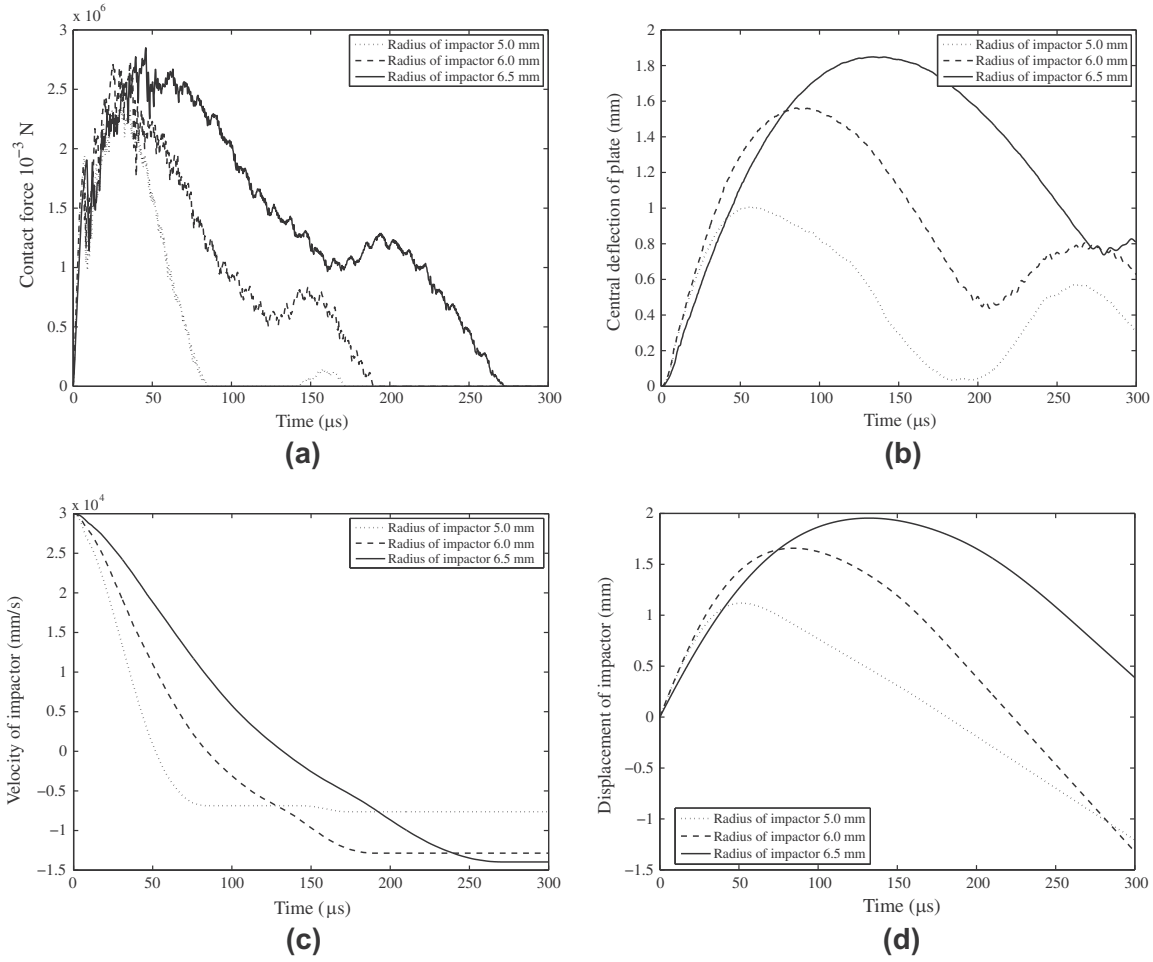

Fig. 14. Influences of the radius of impactor on the impact responses of concentrically stiffened composite laminated plates with the progressive damage analysis model. (a) Contact force; (b) displacement w of plates in contact point, (c) velocity of impactor and (d) displacement of impactor.

The schematic diagram of the LW/SE method for the composite laminated plate with stiffeners impacted by a steel sphere is shown in Fig.1, where the layerwise laminate theory is used to model the behavior of the composite laminated plates, and the traditional solid element is employed to discrete the stiffeners. And then, based on the governing equations of the lamianted plate and stiffeners, the final governing equations of the composite stiffened laminated plate can be assembled by using the interface conditions to ensure the compatibility of displacements at the interface between plate and stiffeners as follow

$$\begin{bmatrix} \boldsymbol{M}_{11}^{P}+\boldsymbol{M}_{11}^{S} & \boldsymbol{M}_{12}^{P} & \boldsymbol{M}_{12}^{S} \\ \boldsymbol{M}_{21}^{P} & \boldsymbol{M}_{22}^{P} & \boldsymbol{0} \\ \boldsymbol{M}_{21}^{S} & \boldsymbol{0} & \boldsymbol{M}_{22}^{S} \end{bmatrix} \begin{Bmatrix} \ddot{\boldsymbol{U}}_{1}^{P} \\ \ddot{\boldsymbol{U}}_{2}^{P} \\ \ddot{\boldsymbol{U}}_{2}^{S} \end{Bmatrix} + \begin{bmatrix} \boldsymbol{K}_{11}^{P}+\boldsymbol{K}_{11}^{S} & \boldsymbol{K}_{12}^{P} & \boldsymbol{K}_{12}^{S} \\ \boldsymbol{K}_{21}^{P} & \boldsymbol{K}_{22}^{P} & \boldsymbol{0} \\ \boldsymbol{K}_{21}^{S} & \boldsymbol{0} & \boldsymbol{K}_{22}^{S} \end{bmatrix} \begin{Bmatrix} \boldsymbol{U}_{1}^{P} \\ \boldsymbol{U}_{2}^{P} \\ \boldsymbol{U}_{2}^{S} \end{Bmatrix} = \begin{Bmatrix} \boldsymbol{0} \\ \boldsymbol{F}_{2}^{P} \\ \boldsymbol{F}_{2}^{S} \end{Bmatrix} \tag{11}$$

where the superscript P and S denote plates and stiffeners, respectively. The subscripts 1 and 2 denote the interface displacements vector and internal displacements vector, respectively. $\boldsymbol{U}$, $\ddot{\boldsymbol{U}}$ and $\boldsymbol{F}$ are the displacements, accelerations and external loads vector, respectively. $\boldsymbol{M}_{ij}^{\alpha}(i,j=1,2;\alpha=S,B)$ is the mass matrixes, $\boldsymbol{K}_{ij}^{\alpha}(i,j=1,2;\alpha=P,S)$ is the stiffness matrixes, and their detailed expressions can be found in [1]. In the present work, the nodes of the stiffeners at the interface are coincide with the nodes of the plate to ensure the fully coordination of displacements and forces at the interface between plate and stiffeners. However, in order to reduce the complexity which results from the consistency requirement of the nodes at the interface, some of the other methods would be employed to deal with this coupling problem in our further works, such as the meshfree method and the tied interface scheme.

Eq. (11) represents a set of ordinary differential equations in time. In order to solve those equations, we must fully discretize them and reduce them to algebraic equations by using a numerical integration method. In present work the Newmark time integration scheme is employed to approximate the time derivatives [59].

The computational algorithm of the contact force between impactor and composite laminated plate can be found in Ref. [21,22]. For the low-impact problem studied in this paper, the initial conditions are $\dot{w}_{\mathrm{i}}^{0}=v_0$ (initial velocity of impactor), $w_{\mathrm{i}}^{0}=w_{\mathrm{t}}^{0}=0$. Firstly, an approximate value of f_{c} is obtained from implicit expressions of the loading law (the first equation of Eq. (6)) by using the initial conditions and a root finding aglorithm, where the Newton–Raphson method is employed. Then, the approximate f_{c}^{1} is now applied as external load at the contact node of laminated plate and the displacement of laminated plate at the contact node w_{t}^{1} is next found from Eq. (11). Using the displacement $w_{\mathrm{t}}^{1}, f_{\mathrm{c}}^{1}$ is recomputed by Eq. (6), as is done previously. This iterative process is repeated till the required accuracy is achieved. The final contact force is now used to calculate acceleration, velocity and displacement of the impactor for the iterative process of the next time step.

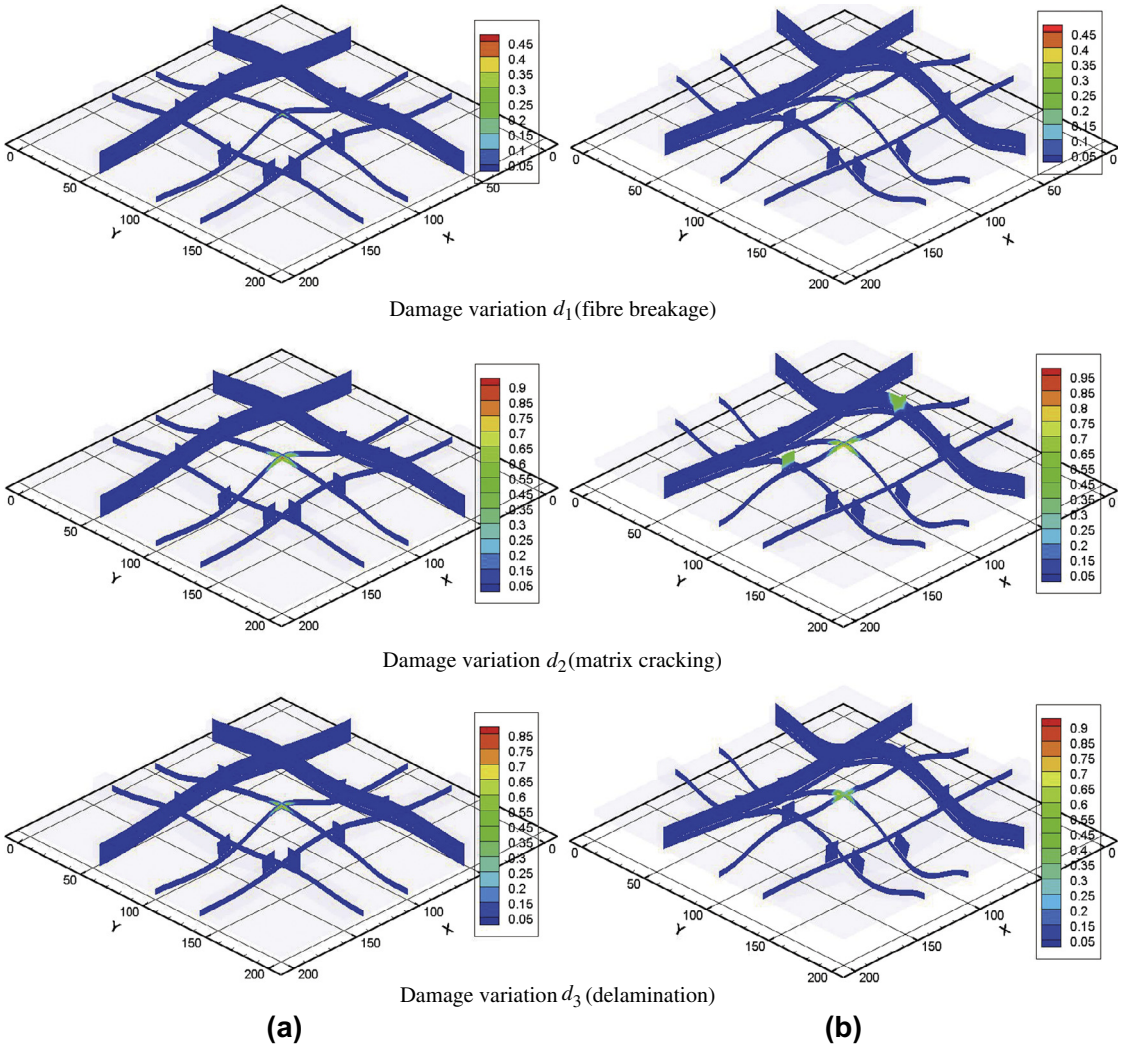

Fig. 15. Influences of the radius of impactor on damage variations distributions of concentrically stiffened composite laminated plates with four stiffeners, where the impact velocity is 30 m/s and the thickness of stiffeners is 7.0 mm. (a) Radius of impactor 5.0 mm; and (b) radius of impactor 7.0 mm.

4. Progressive failure analysis for the impact-induced damage

4.1. Three-dimensional continuum damage model

Distributed microscopic damage is quantified by the use of an appropriate tensor field that describes the orientation and density of microcracks in the material. The microcracks and microvoids cause the cross-sectional area A reducing to $\overline{A}$. The damage variable and effective Cauchy stress can be defined as follows

$$d = (A - \overline{A})/A \tag{12}$$

$$\bar{\boldsymbol{\sigma}} = \boldsymbol{\sigma}/(1-d) \tag{13}$$

where $\boldsymbol{\sigma}$ is the Cauchy stress tensor. However, For the convenience of the finite element equations, Voigt form of the Cauchy stress is used in the other sections. The damage variables d_1, d_2 and d_3, known as three scalar damage parameters, represent modulus reductions under different loading conditions due to microdamage in the material. For fabric plies d_1 and d_2 are associated with damage or failure in the principle fiber directions, and controls in-plane shear damage or failure. The scalar damage parameters d_i represents the effective fractional reduction in load carrying area on planes that are perpendicular to the$i$th principal material direction. In the present work, the first principal material direction is chosen to coincide with the fiber direction. The second principal material direction is chosen to coincide with the transverse direction in lamina plane. The third principal material direction is chosen to coincide with the thickness direction. The scalar damage parameters have values $0 \leqslant d_i \leq 1$, where $d_i = 0$ corresponds to a complete lack of microcracks at the ith principal material direction, while $d_i = 1$ corresponds to a complete separation of the material across planes at the ith principal material direction.

Based on the damage tensor, the effective stress of the orthotropic material with mircodamages can be defined as follows

$$\bar{\boldsymbol{\sigma}} = \boldsymbol{M}_{\mathrm{d}} \cdot \boldsymbol{\sigma} \tag{14}$$

where $\boldsymbol{M}_{\mathrm{d}} = \mathrm{diag}[\,1/\omega_{11} \quad 1/\omega_{22} \quad 1/\omega_{33} \quad 1/\omega_{23} \quad 1/\omega_{13} \quad 1/\omega_{12}\,]$, $\omega_{11} = 1 - d_1,\ \omega_{22} = 1 - d_2,\ \omega_{33} = 1 - d_3,\ \omega_{12} = \sqrt{(1-d_1)(1-d_2)}$, $\omega_{13} = \sqrt{(1-d_1)(1-d_3)}$, $\omega_{12} = \sqrt{(1-d_1)(1-d_2)}$.

According the strain energy for the material without damages, the equivalence strain energy for the damaged orthotropic material is following

$$W_{\mathrm{d}} = \frac{1}{2}\bar{\boldsymbol{\sigma}} \cdot \boldsymbol{C}^{-1} \cdot \bar{\boldsymbol{\sigma}} = \frac{1}{2}\boldsymbol{\sigma} \cdot \boldsymbol{M}_{\mathrm{d}}^{\mathrm{T}} \cdot \boldsymbol{C}^{-1} \cdot \boldsymbol{M}_{\mathrm{d}} \cdot \boldsymbol{\sigma} = \frac{1}{2}\boldsymbol{\sigma} \cdot \left(\boldsymbol{C}^{\mathrm{d}}\right)^{-1} \cdot \boldsymbol{\sigma} \tag{15}$$

where $\boldsymbol{C}^{\mathrm{d}} = \boldsymbol{M}_{\mathrm{d}}^{-1} \cdot \boldsymbol{C}^{-1} \cdot \boldsymbol{M}_{\mathrm{d}}^{-\mathrm{T}}$ is the constitutive of the damaged orthotropic composite laminates.

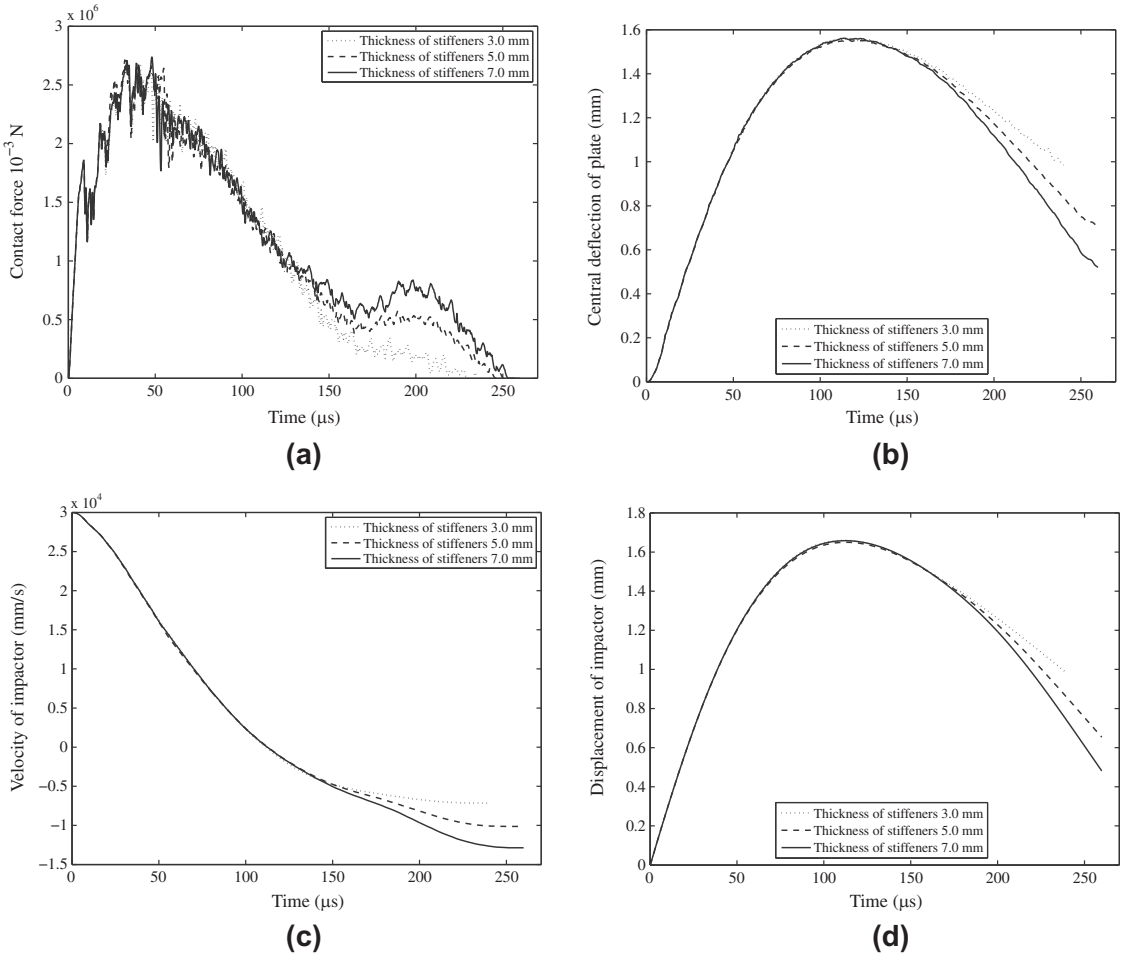

Fig. 16. Influence of the thickness of stiffeners on the impact responses of concentrically stiffened composite laminated plates with the progressive damage analysis model. (a) Contact force; (b) displacement w of plates in contact point, (c) velocity of impactor and (d) displacement of impactor.

4.2. Damage initiation criteria

The failure initiation criteria employed in the present work is 3D Hashin criteria in quadratic strain [63,64], in which failure mode indexes in three principle directions, fiber tension or compression failure F_f, matrix tension or compression failure F_m and delaminations F_z, are defined by

$$F_f^2 = \begin{cases} \left(\frac{\varepsilon_{11}}{\varepsilon_{11}^{f,t}}\right)^2 + \left(\frac{\varepsilon_{12}}{\varepsilon_{12}^{f,t}}\right)^2 + \left(\frac{\varepsilon_{13}}{\varepsilon_{13}^{f,t}}\right)^2 \geqslant 1 & (\varepsilon_{11} > 0) \\ \left(\frac{\varepsilon_{11}}{\varepsilon_{11}^{f,c}}\right)^2 \geqslant 1 & (\varepsilon_{11} < 0) \end{cases} \tag{16}$$

$$F_m^2 = \begin{cases} \left(\frac{\varepsilon_{22}+\varepsilon_{33}}{\varepsilon_{22}^{f,t}}\right)^2 - \frac{\varepsilon_{22}\cdot\varepsilon_{33}}{\left(\varepsilon_{23}^{f}\right)^2} + \left(\frac{\varepsilon_{12}}{\varepsilon_{12}^{f}}\right)^2 + \left(\frac{\varepsilon_{13}}{\varepsilon_{13}^{f}}\right)^2 + \left(\frac{\varepsilon_{23}}{\varepsilon_{23}^{f}}\right)^2 \geqslant 1 & (\varepsilon_{22}+\varepsilon_{33} > 0) \\ \left(\frac{\varepsilon_{22}+\varepsilon_{33}}{\varepsilon_{22}^{f,c}}\right)^2 + \frac{\varepsilon_{22}+\varepsilon_{33}}{\varepsilon_{22}^{f,c}}\left(\frac{\varepsilon_{22}^{f,c}}{2\varepsilon_{12}^{f}} - 1\right) - \frac{\varepsilon_{22}\cdot\varepsilon_{33}}{\left(\varepsilon_{23}^{f}\right)^2} \\ \quad + \left(\frac{\varepsilon_{12}}{\varepsilon_{12}^{f}}\right)^2 + \left(\frac{\varepsilon_{13}}{\varepsilon_{13}^{f}}\right)^2 + \left(\frac{\varepsilon_{23}}{\varepsilon_{23}^{f}}\right)^2 \geqslant 1 & (\varepsilon_{22}+\varepsilon_{33} < 0) \end{cases} \tag{17}$$

$$F_z^2 = \begin{cases} \left(\frac{\varepsilon_{33}}{\varepsilon_{33}^{f,t}}\right)^2 + \left(\frac{\varepsilon_{13}}{\varepsilon_{13}^{f}}\right)^2 + \left(\frac{\varepsilon_{23}}{\varepsilon_{23}^{f}}\right)^2 \geqslant 1 & (\varepsilon_{33} > 0) \\ \left(\frac{\varepsilon_{33}}{\varepsilon_{33}^{f,c}}\right)^2 + \left(\frac{\varepsilon_{13}}{\varepsilon_{13}^{f}}\right)^2 + \left(\frac{\varepsilon_{23}}{\varepsilon_{23}^{f}}\right)^2 \geqslant 1 & (\varepsilon_{33} < 0) \end{cases} \tag{18}$$

where $\varepsilon_{ii}^{f,t} = \sigma_{ii}^{f,t}/C_{ii}$, $(i = 1,2,3)$; $\varepsilon_{ii}^{f,c} = \sigma_{ii}^{f,c}/C_{ii}$, $(i = 1,2,3)$; $\varepsilon_{12}^{f} = \sigma_{12}^{f}/C_{66}$; $\varepsilon_{23}^{f} = \sigma_{23}^{f}/C_{44}$; $\varepsilon_{13}^{f} = \sigma_{13}^{f}/C_{55}$. $\sigma_{ii}^{f,t}$ and $\sigma_{ii}^{f,c}$ are the tensile and compression strength of three principle directions of material, respectively; σ_{12}^{f}, σ_{13}^{f} and σ_{23}^{f} are shear strength in three planes of material.

4.3. Damage evolution law

In a finite-element-based failure analysis procedure, an element failure is first identified through the use of one of the above failure criteria and later through a stiffness reduction scheme. The failed element is replaced with an equivalent element according a material property degradation model. A number of post-failure material property degradation models have been proposed for the progressive failure analysis. Most of these material degradation models belong to one of three general categories [65,66]: instantaneous unloading, gradual unloading and constant stress at failure material point. In instantaneous unloading scheme the selected material properties of the failure element are reduced to zero when the failure is detected. One of the most common instantaneous unloading categories used for degradation of material properties is the ply-discount theory for composite structures. This kind stiffness degradation scheme is independent of the mesh form used in the analysis. However, it may be noted that the size of the actual damage in the form of micro or meso cracks is very small compared to the size of the elements. Hence it appears unjustified in reducing

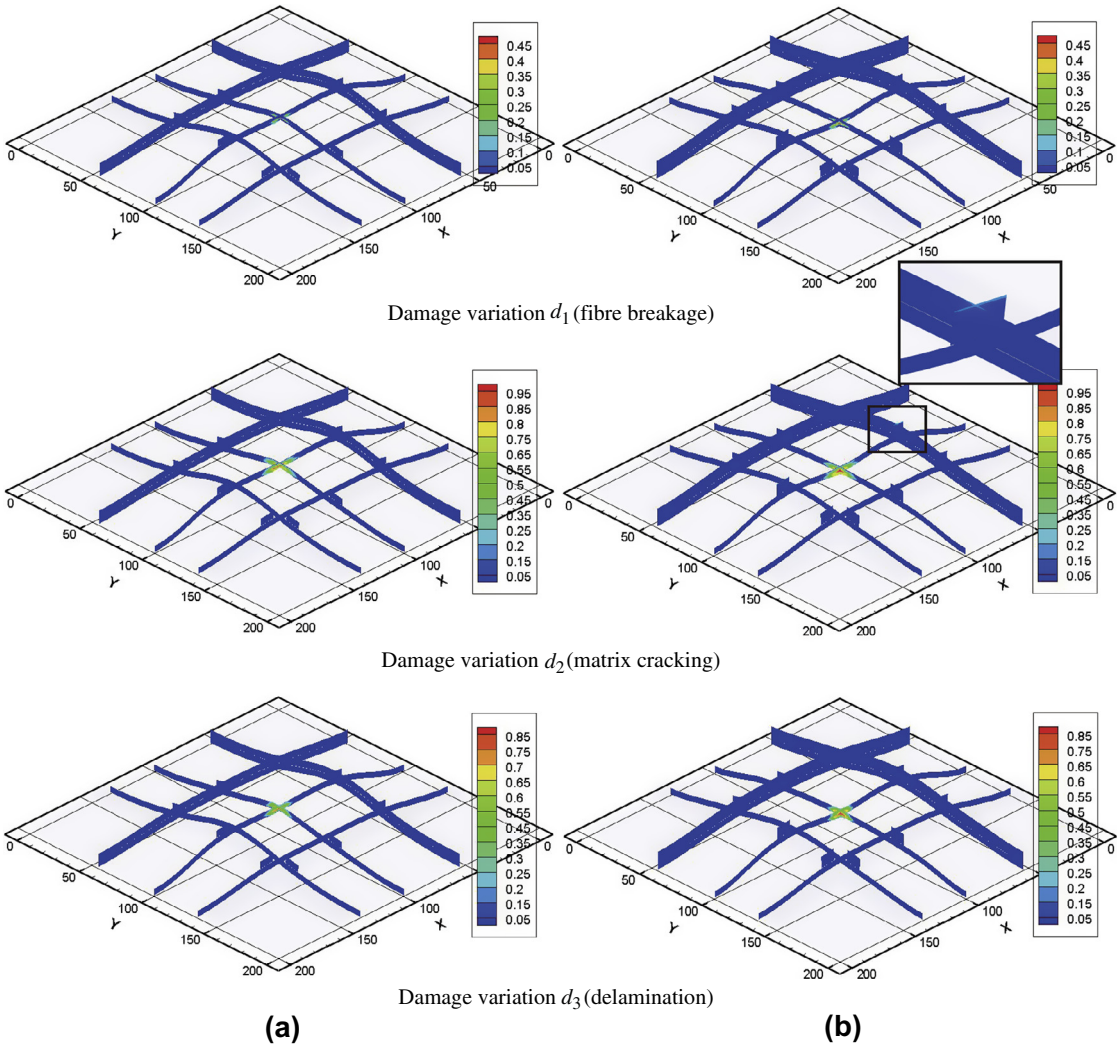

Fig. 17. Influences of thickness of stiffeners on damage variations distributions of concentrically stiffened composite laminated plates with four stiffeners, where the impact velocity is 30 m/s and the radius of impactor is 6.0 mm. (a) Thickness of stiffeners 3.0 mm; and (b) thickness of stiffeners 5.0 mm.

the stiffness properties of the whole element to zero. For the constant stress case, the material properties associated with that mode of failure are degraded such that the material cannot sustain additional load. For the gradual unloading case, the material property associated with that mode of failure is degraded gradually (exponentially for example) until it reaches zero, and the degradation can be either independent or interactive corresponding to the mode of failure.

In the present work, the reduction of the stiffness coefficients is controlled by damage variables d_1, d_2 and d_3 which take values between zero (undamaged state) and one (fully damaged state for the mode corresponding to this damage variable). The gradual unloading scheme of damage variables d_1, d_2 and d_3 can be divided into two types: linear and nonlinear. For the nonlinear type, the damage variable is given as follows

$$d_1 = 1 - \frac{\exp\left[-\sigma_{11}^{f}\delta_{eq,11}^{f}(F_f - 1)/G_{c,1}\right]}{F_f}$$
$$d_2 = 1 - \frac{\exp\left[-\sigma_{22}^{f}\delta_{eq,22}^{f}(F_m - 1)/G_{c,2}\right]}{F_m} \quad (19)$$
$$d_3 = 1 - \frac{\exp\left[-\sigma_{33}^{f}\delta_{eq,33}^{f}(F_z - 1)/G_{c,3}\right]}{F_z}$$

where $G_{c,1}$, $G_{c,2}$ and $G_{c,3}$ are the fracture energy of three principle directions of material, respectively. $\delta_{eq,11}^{f}$, $\delta_{eq,22}^{f}$ and $\delta_{eq,33}^{f}$ are the equivalent displacements at which the material is fully damaged.

$$\delta_{eq,ii}^{f} = \varepsilon_{ii}^{f} \cdot L_c \quad (20)$$

where L_c is a characteristic length of the element. Different methods have been suggested for computing the characteristic length. Bazant and Oh [67] proposed the following relation for square element:

$$L_c = \frac{\sqrt{A_{IP}}}{\cos\theta} \quad (21)$$

where A_{IP} is the area associated with an integration point and θ is the angle between the mesh line along which the crack band advances and the crack direction. According to Maimi [68], for an unknown direction of crack propagation the average of above expression can be used, $\bar{L}_c = \frac{\pi}{4}\int_0^{\pi/4} L_c d\gamma = 1.12\sqrt{A_{IP}}$. Lapczyk and Hurtado [69] assumed that the characteristic length at a material point is equal to the square root of the area associated with it, although any other of the methods mentioned previously could be incorporated easily in the model.

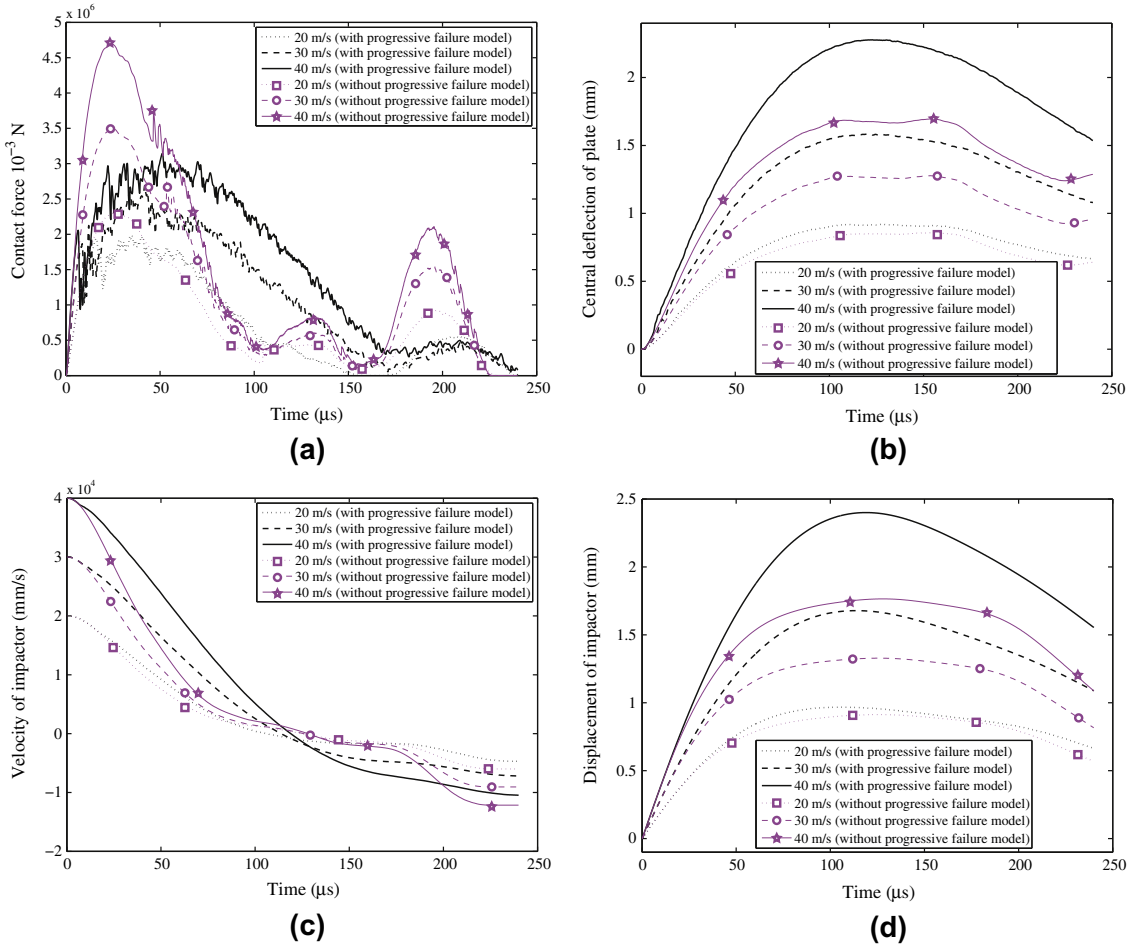

Fig. 18. Influence of the impact velocity on the impact responses of parallelly stiffened composite laminated plates with/without the progressive damage analysis model. (a) Contact force; (b) displacement w of plates in contact point, (c) velocity of impactor and (d) displacement of impactor.

5. Numerical examples

5.1. Validation of the present method

Example 1. Validation of the current finite element code has been carried out by the same example as that used in many other literatures [9,70,10]. A simply supported graphite/epoxy composite plate [0/90/0/90/0]s of the dimensions 200 mm × 200 mm × 2.69 mm is impacted by a steel sphere of 12.7 mm diameter at a velocity of 3 m/s. All the layers of the laminated plate have the same thickness and material properties.

$E_{11} = 141.2\,\text{GPa}$, $E_{22} = 9.72\,\text{GPa}$, $G_{12} = 5.53\,\text{GPa}$, $G_{23} = 3.74\,\text{GPa}$, $v_{12} = v_{23} = 0.30$, $\rho = 1536\,\text{Kg/m}^3$

The uniform and nonuniform finite element scheme are presented in Fig. 2, where the nonuniform elements are to refine the local grid in the area of impact point. Convergence of the contact force, the displacement w of the plate at the contact point, the velocity of the impactor and the indentation depth of the plate are shown in Fig. 3, where the finite elements are uniformly distributed. It can be seen from Fig. 3 that the responses of impact converge to the value of mathematical model monotonically as the number of the finite elements increased. The reasonable convergence values are achieved when the finite elements scheme is 1600(40×40). The contact force, the displacement w of plate at the contact point, the residual velocity of impactor and the indentation increase with the increasing of the number of the finite elements. It suggests that the stiffness of composite laminated plate decreases and the secondary impact delays with the increasing of the number of the finite elements. For the nonuniform discretization (see Fig. 2), convergence of the contact force, the displacement w of plate at the contact point, velocity of impactor and indentation of plate are shown in Fig. 4. It can be observed from Fig. 4 that the convergence rate of the maximum contact force of the first loading–unloading cycle is improved significantly by the nonuniform finite element scheme. However, it almost has no effect on the convergence rate of the contact force peak value and starting time of the secondary impact. Therefore, the nonuniform finite element scheme could reduce the computational cost for the evaluation of impact-induced damage, since the damage of the low-impact is caused in the first impact periods. But if the complete impact responses are needed, there is no difference between the uniform and nonuniform finite element schemes.

Comparison of the contact force and the deflection histories obtained by the present method with the results obtained by other literatures [9,70,10] are shown in Fig. 5. It may be seen in Fig. 5 that the contact force history and the time history of the central deflection obtained by the current finite element code are in reasonable agreement with the results reported in previous investigations.

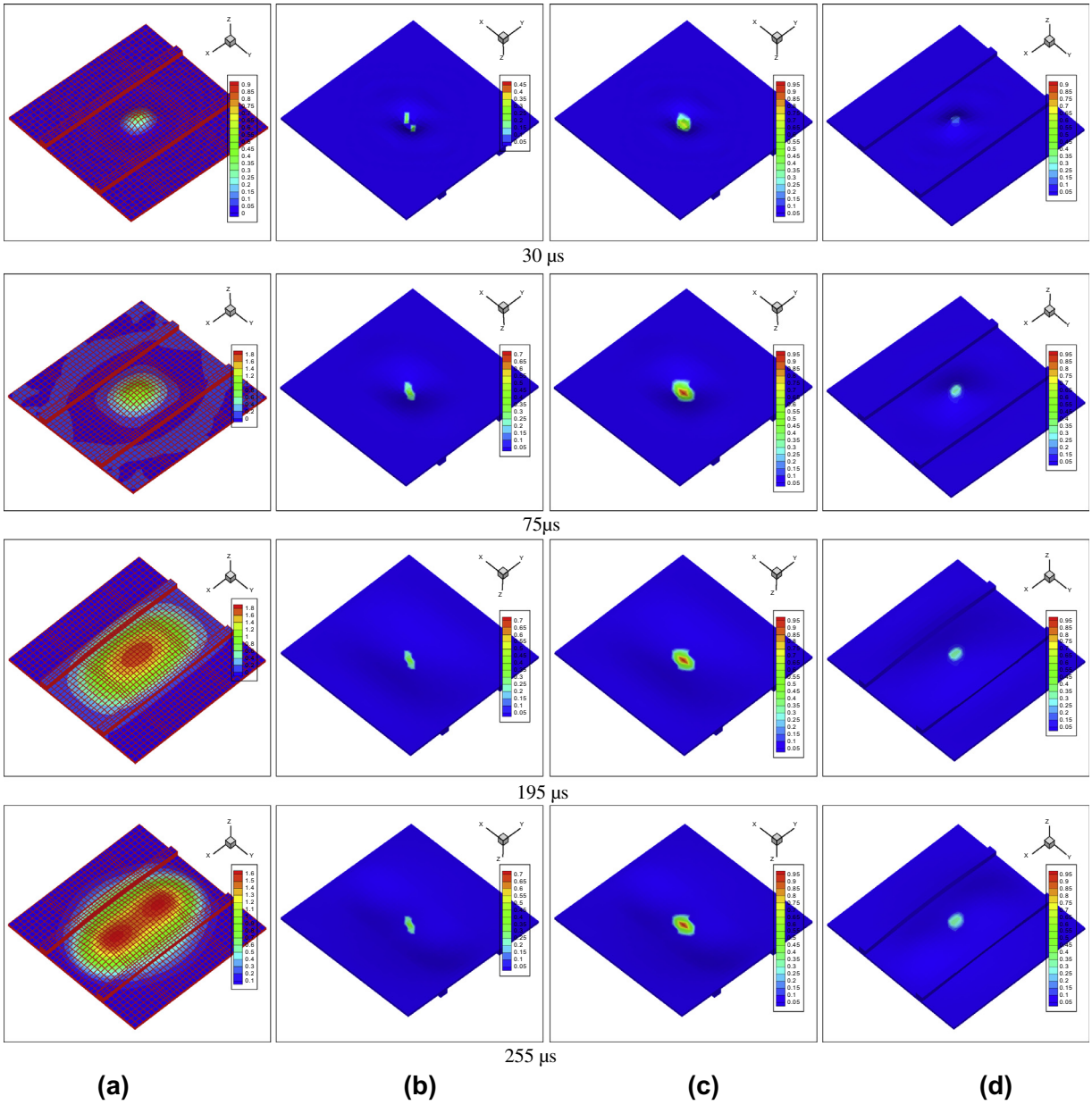

Fig. 19. The deflection and damage variations histories of parallelly stiffened composite laminated plates subjected to impact velocity 40 m/s. (a) Deflection and nephogram of displacement w; (b) damage variation d_1 (fiber breakage); (c) damage variation d_2 (matrix cracking); and (d) damage variation d_3 (delamination).

Example 2. The composite laminated plate studied in this numerical example have the same geometry as in Example 1. But the stacking sequence is [0/90/0/90/0], and the density $\rho = 1389.2\ \mathrm{Kg/m^3}$. Material properties of the composite laminates are listed in Table 1 [71].

A number of investigations have demonstrated that upon impact by a low velocity, the main part of damage in the composite laminates is caused by matrix cracking and delaminations, because the tensile failure strength of the fiber is high, and the damage induced by fiber breakage is generally very limited and confined to the region under and near the contact area between the impactor and the laminates. Choi et al. [17] reported that intraply matrix cracking is the initial damage mode, and the delamination damage initiates once the matrix crack reaches the interface between the ply groups having different fiber orientaions after propagating throughout the thickness of the ply group consisting of the cracked ply.

If the three-dimensional theory of plate and Herlz's theory are employed to analyze the low velocity impact problem, first we need to determine the load application point of the equivalent contact force in thickness direction. The major aim of this numerical example is to investigate the effect of the load application point of the equivalent contact force in thickness direction on the impact responses. The impact responses of composite laminated plate with/without the progressive damage analysis model are shown in Fig. 6, where the initial velocity of the impactor is 30 m/s and the radius of the impactor is 6.0 mm. Because the material property associated with the failure is degraded gradually when the failure is detected, the maximum of the contact force, the central deflection of plate at middle surface and the displacement of the impactor without tht progressive failure model are greater than those with the progressive failure model. It can be seen from Fig. 6 that the load point in thickness direction has no effect on the impact responses except the maximum contact force of the

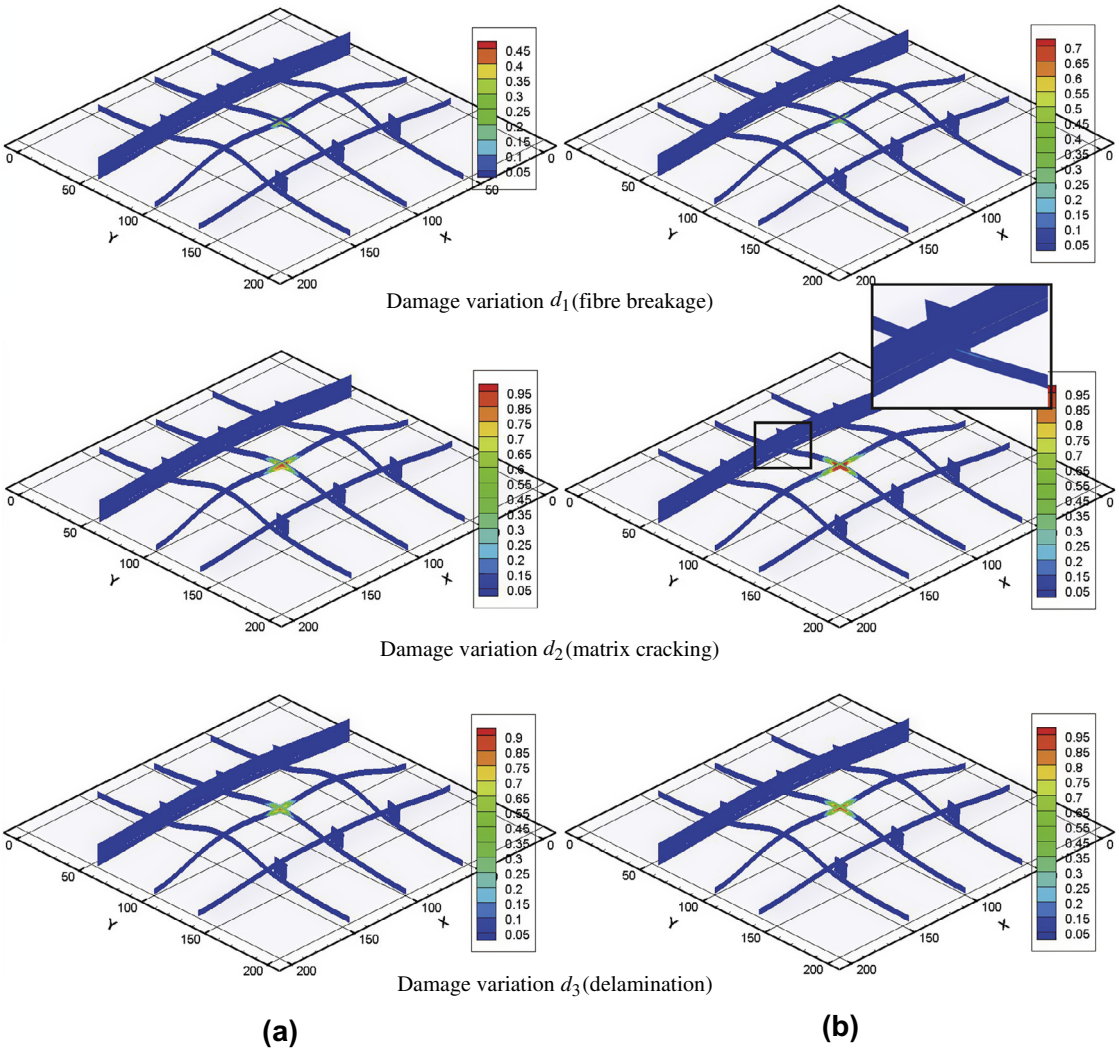

Fig. 20. Influence of impact velocity on damage variations distributions of parallelly stiffened laminated plate with two stiffeners, where the radius of impactor 6.0 mm and the thickness of stiffeners is 7.0 mm. (a) Impact velocity 30 m/s; and (b) impact velocity 40 m/s.

secondary impact if the impact-induced damage is not taken into account, while with the progressive damage model the load point in thickness direction has significant influence on the impact responses. One important reason is that the impact-induced damage always initiates from area nearby the load point since the contact force is equivalent to a point load in the low velocity impact analysis method estiblished by Hertz's low.

The deflection and damage variations of the composite laminated plate subjected to impact load on the lower surface, the middle surface and the upper surface are shown in Figs. 7–9, respectively. Initial times of the fiber breakage, matrix cracking and delaminations are listed in Table 2. It can be observed from Figs. 7–9 and Table 2 that the matrix cracking and delaminations are the main part of damage in the composite laminates, and the damage variation of fiber breakage is much smaller than those of matrix cracking and delaminations and confined to the region near the contact area. The matrix cracking is the initial damage mode, and then the delamination damage initiates, at last the fiber breakage propagates. When the equivalent point load resulted from impact is located on the lower surface, the impact-induced damage initiates and develops from the lower surface of laminated plate. Athougth the fiber damage confined to the region under and near the contact area between the impactor and the laminates is logical, it is not resonable for the matrix cracking and delamination which are the main part of damage. When the equivalent point load resulted from impact is located on the upper surface, the impact-induced damages are initiated and developed on the upper surface of laminated plate. It is not reasonable for three kinds of damages. In contrast, when the equivalent point load resulted from impact is located on the middle surface, the initiation and development of the matrix cracking and delamination are along the thickness direction of laminated plate. Although the fiber damage initiated and developed on the middle region of thickness direction is not resonable, it is not the main part of damage and does not influence the impact responses significantly. Therefore, in the numerical examples of the next sections the equivalent point load resulted from impact is acted on the middle surface of laminated plates.

5.2. Composite laminated plates with stiffeners

The response of stiffened structures is affected significantly by the form and distribution of stiffeners. Therefore, two kinds of stiffened composite laminated plates (see Fig. 10) are investigated in this section, concentrically stiffened laminated plates with four stiffeners and parallelly stiffened laminated plates with two stiffeners. The influence of different parameters of the stiffeners and

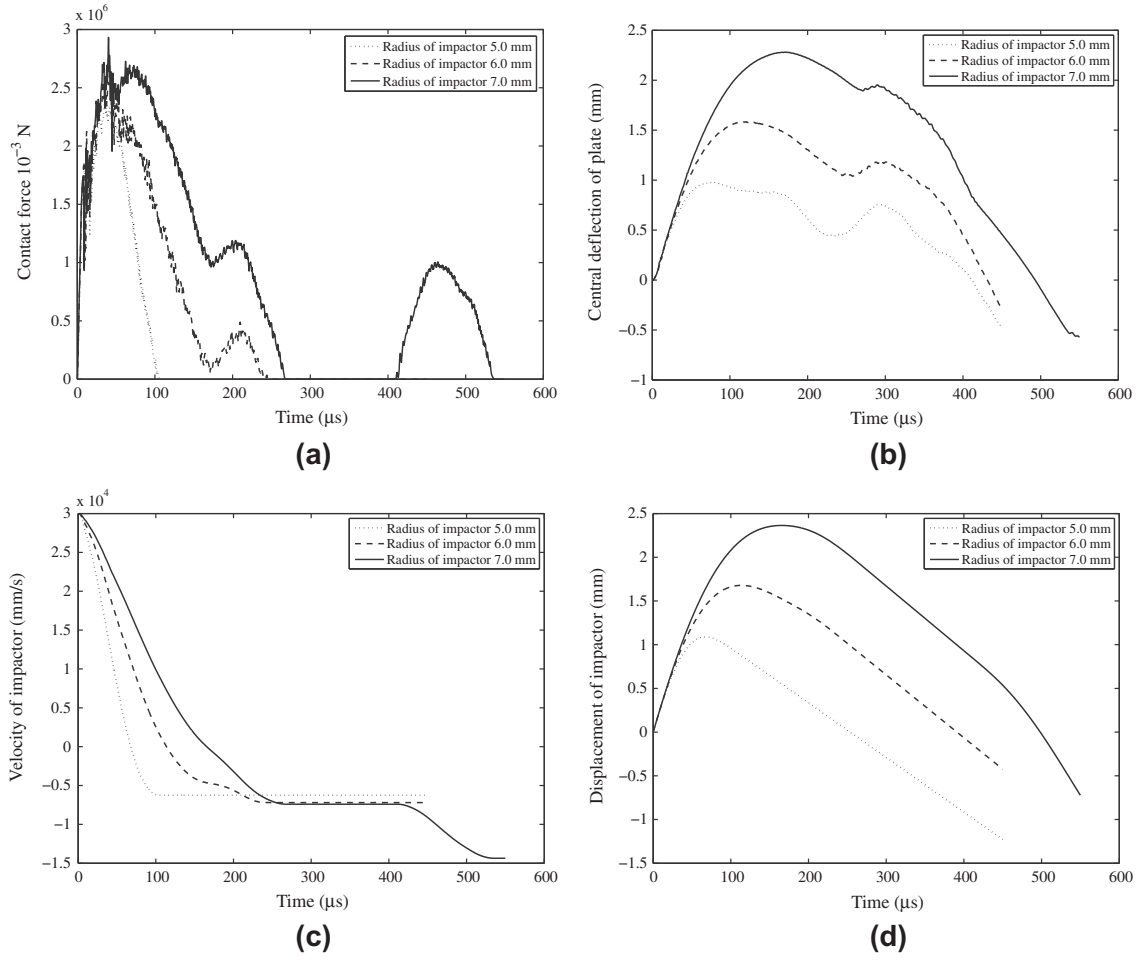

Fig. 21. Influence of the radius of impactor on the impact responses of parallelly stiffened composite laminated plates with the progressive damage analysis model. (a) Contact force; (b) displacement w of plates in contact point, (c) velocity of impactor and (d) displacement of impactor.

impactor, such as the size and form of stiffeners, impact velocity, and the mass of impactor, on the responses and damages is studied as well.

All the layers of laminated plate and stiffeners have same material properties as those listed in Table 1. The stacking sequence of laminated plate is [0/90/0/90/0] and the stacking sequence of stiffeners is [0]. All the single layers of laminated plate have the same thickness. The stiffened composite laminated plates are subjected to low velocity impact at the lower surface, but the load application point of the equivalent contact force is subjected at the middle surface. The density of the impactor is 7960 Kg/m^3. When the effect of the impact velocity on the responses and damages is investigated, the radius of impactor is 6.0 mm and the thickness of stiffeners is 7.0 mm. When the effect of the impact mass (radius of impactor) on the responses and damages is investigated, the impact velocity is 30 m/s and the thickness of stiffeners is 7.0 mm. When the effect of the thickness of stiffeners on the responses and damages is investigated, the radius of impactor is 6.0 mm and the impact velocity is 30 m/s.

5.2.1. Concentrically stiffened laminated plate with four stiffeners

The impact responses of concentrically stiffened composite laminated plates subjected to different impact velocities with/without the progressive damage analysis model are shown in Fig. 11, where the radius of impactor is 6.0 mm and the thickness of stiffeners is 7.0 mm. It is observed that with the increase of impact velocity the effect of the progressive damage analysis model on the responses of plate and impactor increased. Therefore, damage analysis model is necessary for the impact responses analysis problem when the impact velocity is larger. With the increase of the impact velocity, the maximum contact force, the impact completion time, the central deflection of plate and the displacement of impactor also increased. In the first loading–unloading cycle, the contact force fluctuated greatly, especially in the loading phase, because the impact-induced damages are mainly produced in this period.

The deformation and damage histories of the concentrically stiffened composite laminated plates subjected to impact velocity 35 m/s are shown in Fig. 12, where the radius of impactor is 6.0 mm and the thickness of stiffeners is 7.0 mm. The influences of the impact velocity on damage variations distributions is shown in Fig. 13, where the damage variations distributions are the final results after the impact. It is observed that in the early stages of impact the deformation of laminated plate is limited in the rectangular region surrounded by four stiffeners, and then with the elastic resilience the deformation of laminated plate began to expand out the rectangular region surrounded by stiffeners. In the process of the impact, the fiber breakage is generally very limited ($d_1 < 0.45$) and confined to the region near the contact area between the impactor and the laminates. Serious matrix cracking and delamination arised near the contact region are the main part of damage in the composite laminates. The fiber breakage and

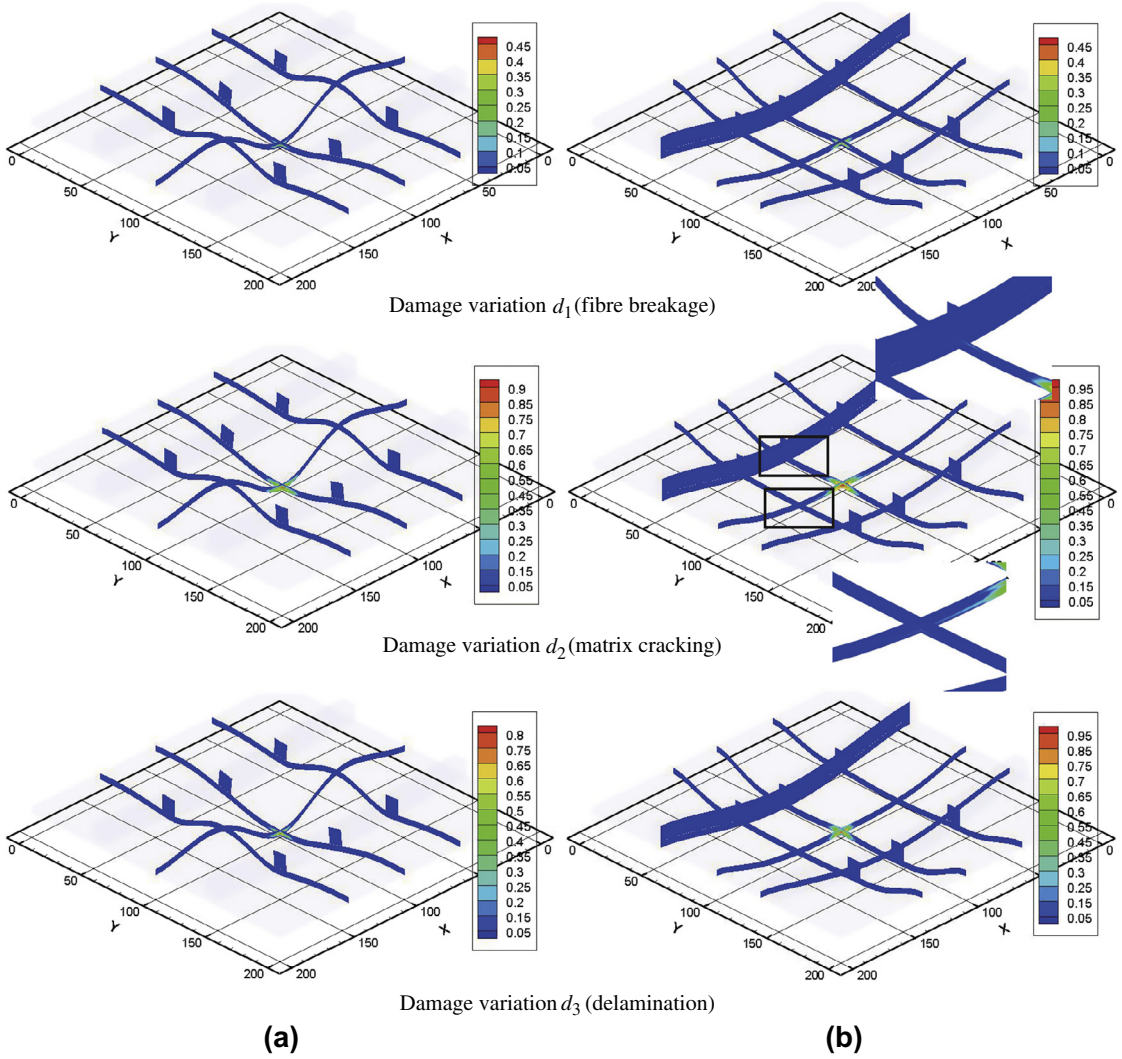

Fig. 22. Influence of radius of impactor on damage variations distributions of parallelly stiffened laminated plate with two stiffeners, where the impact velocity is 30 m/s and the thickness of stiffeners is 7.0 mm. (a) radius of impactor 5.0 mm; and (b) radius of impactor 7.0 mm.

delaminations are mainly induced in the first loading–unloading cycle, while the matrix failure is extending constantly to far away from the contact area especially the middle of the *x*-direction (fiber direction) stiffeners and the interface region between the *y*-direction stiffeners and laminated plate (see the second subgraph of Fig. 13(b)). Because the stacking sequence of laminated plate is [0/90/0/90/0] and stacking sequence of stiffeners is [0], the stiffness of the stiffened composite laminated plate in the fiber direction (*x*-direction) is greater than stiffness in the transverse direction (*y*-direction). It results in that the deflection of laminated plate and stiffeners in the *y*-direction is larger than that in the *x*-direction, which is the reason why the impact-induced damages tend to spread to the middle of the *x*-direction stiffeners and the interface region between the *y*-direction stiffeners and laminated plate. Consequently, there are three danger zones for the concentrically stiffened composite laminated plates subjected to low velocity impact: (a) the contact region between impactor and laminated plate; (b) the middle region of the stiffeners along the direction with the weaker stiffness; and (c) the interface region between the laminated plate and the stiffeners along the direction with the stronger stiffness.

With the increase of impact velocity, the values and distribution range of the fiber breakage and the delamination increased along the lower surface of the lamianted plate near the contact area. While the values and distribution range of the matrix cracking not only increased along the lower surface with the increase of impact velocity, but also appeares at the upper surface near the interface region between the *y*-direction stiffeners and laminated plate (see the second subgraph of Fig. 13(b)). In addition, the values and distribution range of the matrix cracking in the*x*-direction stiffeners increased and extanded rapidly.

The influences of the radius of impactor on the impact responses of the concentrically stiffened composite laminated plates with the progressive damage analysis model are shown in Fig. 14, where the impact velocity is 30 m/s and the thickness of stiffeners is 7.0 mm. And the influences of the radius of impactor on damage variations distributions is shown in Fig. 15. It is observed that the radius of impactor has significant influence on the impact responses of the concentrically stiffened laminated plate and impactor since both of the mass and constant of the Hertz's contact theory (see Fig. 3) increased with the increase of the radius of impactor. With the increase of the radius of impactor, the contact force, the impact completion time, the central deflection of plate and the displacement of impactor increased rapidly. The values and distribution range of the fiber breakage, the matrix cracking and the delaminations rapidly increased and extanded with the increase of the radius of impactor.

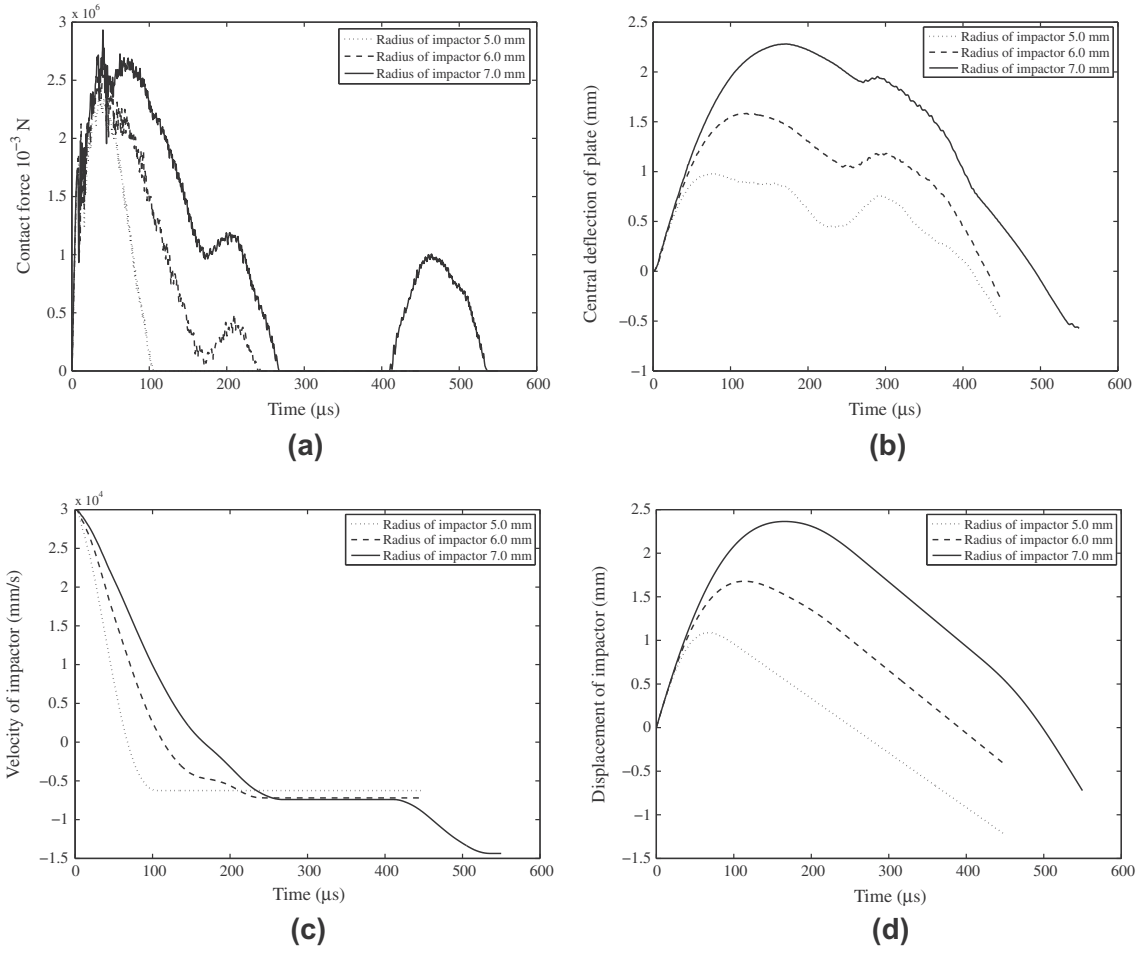

Fig. 23. Influence of the thickness of stiffeners on the impact responses of parallelly stiffened composite laminated plates with the progressive damage analysis model. (a) Contact force; (b) displacement w of plates in contact point, (c) velocity of impactor and (d) displacement of impactor.

Influences of the thickness of stiffeners on the impact responses of the concentrically stiffened composite laminated plates with the progressive damage analysis model are shown in Fig. 16, where the radius of impactor is 6.0 mm and the impact velocity is 30 m/s. It is observed that the thickness of stiffeners has no effect on the impact responses during the first loading–unloading cycle. The reason may be that in the first loading–unloading cycle (the early stages of impact) the deformation of plate is limited in the rectangular region surrounded by four stiffeners. With the increase of thickness of stiffeners, the maximum contact force of the second loading–unloading cycle, the impact completion time and the residual velocity of impactor increased.

Influences of thickness of stiffeners on damage variations distributions of the concentrically stiffened composite laminated plates with four stiffeners are shown in Fig. 17. With the increase of the thickness of stiffeners, the range of the fiber breakage and delaminations increased. The reason is that the increase of the thickness of stiffeners results in the increase of the overall stiffness of the stiffened composite laminated plate. However, the range of the matrix cracking in the y-direction stiffeners first increased and then decreased with the increase of the thickness of stiffeners (see Figs. 13(a) and 17).

5.2.2. Parallelly stiffened laminated plate with two stiffeners

For the parallelly stiffened composite laminated plates, influences of the impact velocity on the impact responses with/without the progressive damage analysis model are shown in Fig. 18, where the radius of impactor is 6.0 mm and the thickness of stiffeners is 7.0 mm. It can be seen from Fig. 18 that with the increase of the impact velocity the effect of the progressive damage analysis model on the responses of laminated plate and impactor increasesed. The contact force increased with the increase of the impact velocity, and the influence of the impact velocity on contact force during the first loading–unloading cycle is more significant than that during the second impact. The deflection of laminated plate and the displacement of impactor increased proportionately as the impact velocity increased.

The deformation and damage variations histories of the parallelly stiffened composite laminated plates with two stiffeners subjected to impact velocity 40 m/s are shown in Fig. 19, where the radius of impactor is 6.0 mm and the thickness of stiffeners is 7.0 mm. Influences of impact velocity on damage variations distributions of the parallelly stiffened laminated plate are shown in Fig. 20. In the early stages of impact the deformation of plate is limit in the rectangular region between two parallelly stiffeners in the x direction, and then with the elastic resilience the deformation of plate began to expand out this region. The extent of the damage (the value of damage variations) and range increased as the impact velocity increased.

The fiber breakage is very limited and confined to the region near the contact area between the impactor and the laminates. The matrix cracking initiates at the contact point, and rapidly expand during the first loading–unloading cycle in the area near the contact point. With the elastic resilience the matrix cracking continued to extend along the lower surface during the second impact. The matrix cracking firstly appears at the upper surface near

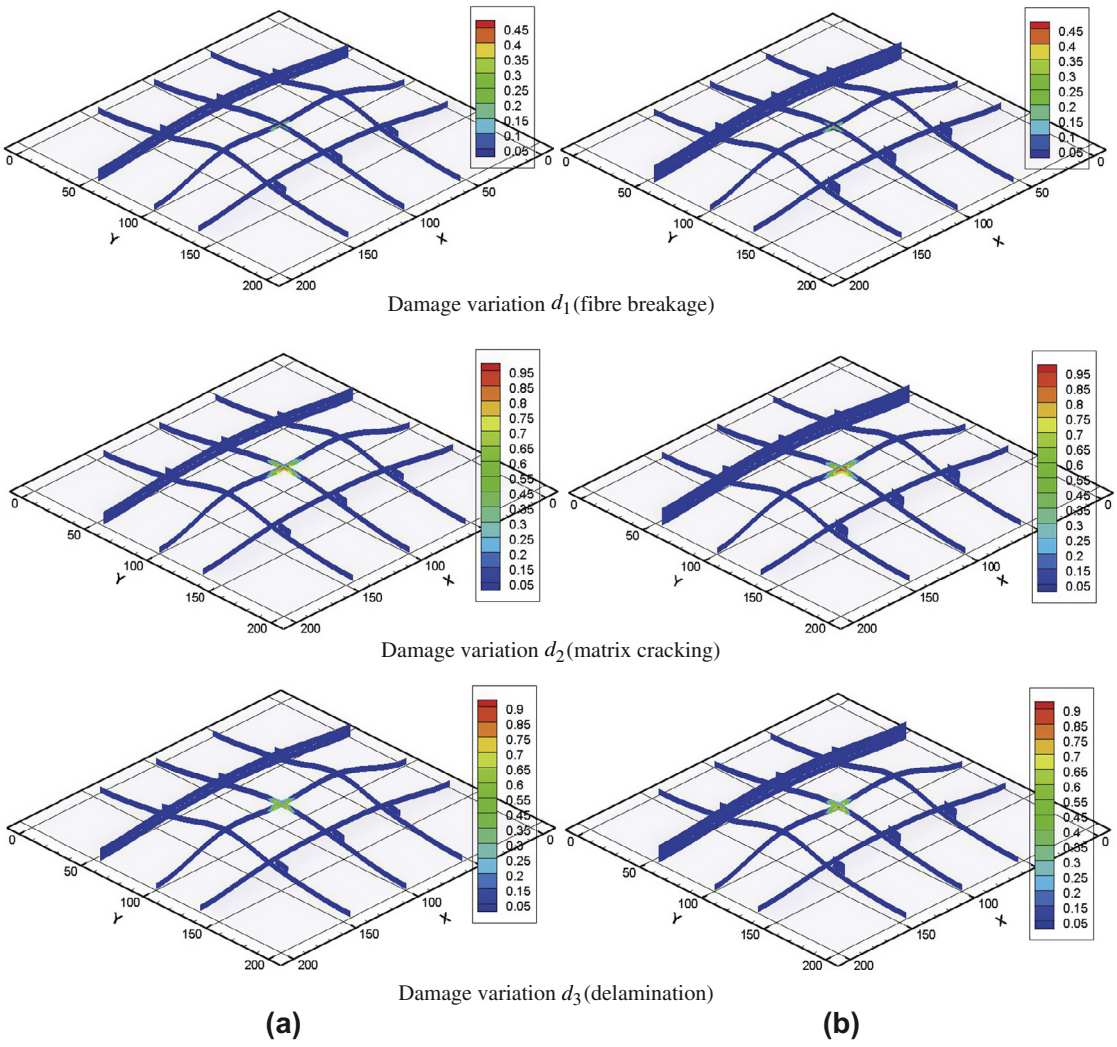

Fig. 24. Influence of thickness of stiffeners on damage variations distributions of parallelly stiffened laminated plate with two stiffeners, where the impact velocity is 30 m/s and the radius of impactor is 6.0 mm. (a) Thickness of stiffeners 3.0 mm; and (b) thickness of stiffeners 5.0 mm.

Table 3
Effects of the parameters on the residual velocity for the concentrically stiffened plate and the parallelly stiffened plate.

	Concentrically stiffened plate		Parallelly stiffened plate	
	v_r	$v_r/v_0 \times 100$	v_r	$v_r/v_0 \times 100$
Initial velocity (m/s)				
20	8.3303	41.6515	4.7011	23.5155
30	12.8645	42.8817	7.1945	23.9817
40 (35)	15.2766	43.6474	10.4774	26.1935
Radius of impactor (mm)				
5.0	7.6256	25.4187	6.2506	20.8353
6.0	12.8645	42.8817	7.1945	23.9817
7.0 (6.5)	13.9746	46.5820	14.3573	47.8577
Thickness of stiffeners (mm)				
3.0	7.1551	23.8503	5.4546	18.1820
5.0	10.1293	33.7643	6.3986	21.3287
7.0	12.8645	42.8817	7.1945	23.9817

the interface between laminated plate and stiffeners and then the it initiates at the lower surface (see Fig. 20(b)). The delamination also initiates at the contact point, and rapidly expand during the first loading–unloading cycle in the area near the contact point. There are two danger zones for the parallelly stiffened composite laminated plates subjected to low velocity impact: (a) the contact region between impactor and laminated plate; and (b) the interface region between the laminated plate and the stiffeners along the direction with the stronger stiffness.

The influences of the radius of impactor on the impact responses of the parallelly stiffened composite laminated plates are shown in Fig. 21, where the impact velocity is 30 m/s and the

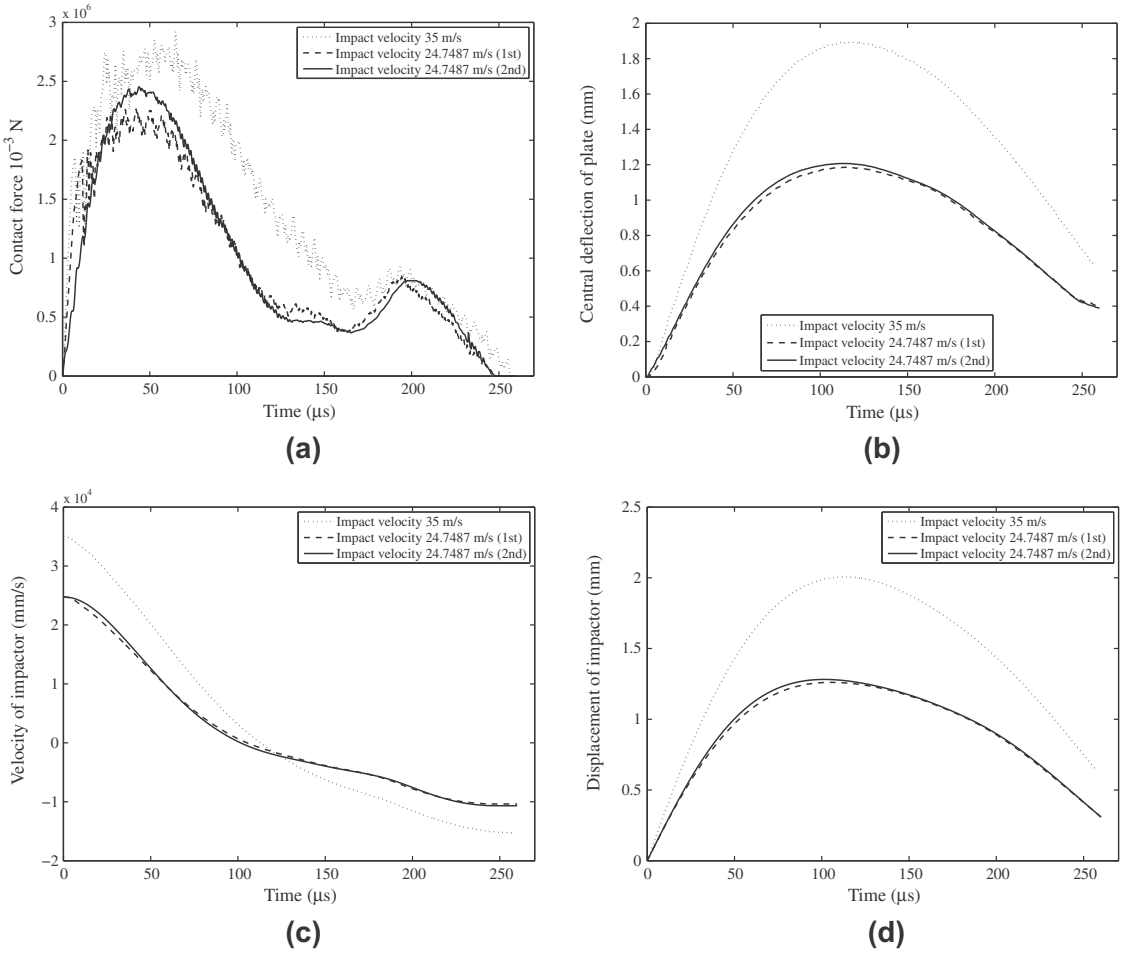

Fig. 25. Impact responses of concentrically stiffened composite laminated plates subjected to multi-impacts. (a) Contact force; (b) displacement w of plates in contact point, (c) velocity of impactor and (d) displacement of impactor.

thickness of stiffeners is 7.0 mm. And the influences of radius of impactor on damage variations distributions are shown in Fig. 22. It is observed that the radius of impactor has also significant influence on the impact responses of the parallelly stiffened laminated plate and impactor. With the increase of the radius of impactor, the contact force, the impact completion time, the central deflection of plate and the displacement of impactor increased rapidly. The values and distribution range of the fiber breakage, the matrix cracking and the delamination rapidly increased and extanded with the increase of the radius of impactor.

Influences of the thickness of stiffeners on the impact responses of the parallelly stiffened composite laminated plates with the progressive damage analysis model are shown in Fig. 23, where the radius of impactor is 6.0 mm and the impact velocity is 30 m/s. Similar to the concentrically stiffened composite laminated plates, the thickness of stiffeners of the parallelly stiffened composite laminated plates has not effect on the impact responses during the first loading–unloading cycle, and the peak value of the second impact increased with the increase of the thickness of stiffeners.

Influences of thickness of stiffeners on damage variations distributions of the parallelly stiffened laminated plate are shown in Fig. 24. It can be seen from Fig. 24 that the thickness of stiffeners of the parallelly stiffened composite laminated plates has a great influence on the fiber breakage and matrix cracking, while the delamination increased slightly with the increase of the thickness of stiffeners.

Effects of the parameters on the residual velocity of the impactor v_r for the concentrically stiffened plate and the parallelly stiffened plate are listed in Table 3, where the values in the brackets are adopted for the concentrically stiffened composite laminated plate. It can be seen from Table 3 that the percentages of the residual velocity in the initial velocity v_0 are increased with the increasing of the initial velocity, the radius of the impactor and the thickness of stiffeners. The percentages of the residual velocity in the initial velocity of the concentrically stiffened plate are larger than that of the parallelly stiffened plate, so the absorption capacity of the impact energy of the parallelly stiffened plate is better than that of the concentrically stiffened plate. Comparing two kinds of stiffened composite laminated plates studied in this section, the deflection of the concentrically stiffened composite laminted plate at the contact point is smaller than that of the parallelly stiffened compoiste laminated plate, while the impact-induced damages just the opposite. Therefore, the impact resistant ability and the stiffness of the stiffened composite laminated plate are contradictory.

5.3. Multi-impacts on stiffened composite laminated plate

Internal damages arised due to low-speed impact event can reduce the residual strength of composite structures significantly. Furthermore, such kind internal damage as delamination and fiber breakage are imperfections. This results in a reduction in stiffness and strength and consequent progagation under further loading.

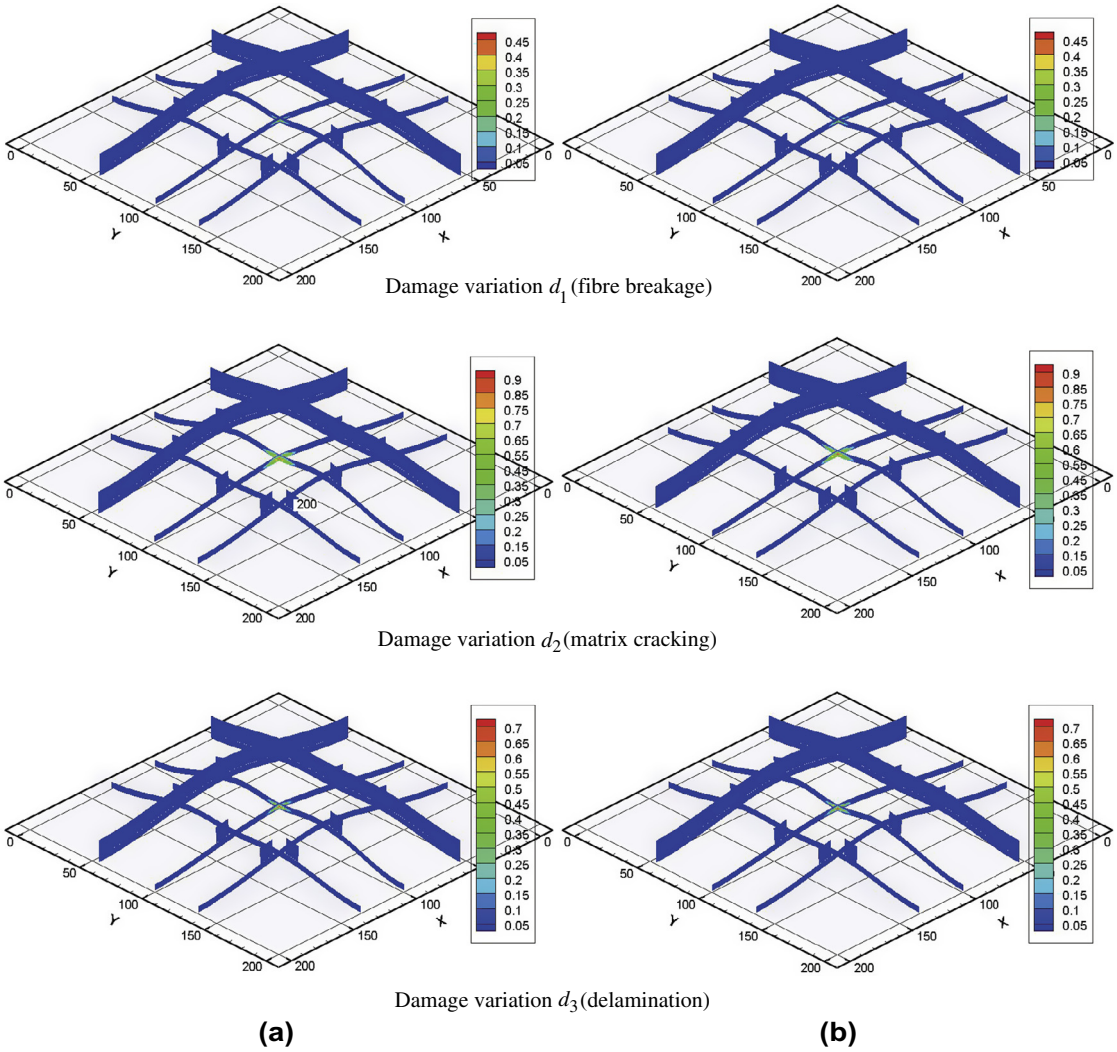

Fig. 26. Damage variations distributions of concentrically stiffened laminated plate subjected to multi-impacts. (a) First impact; and (b) second impact.

The accumulation of these flaws over time may result in failure of the apparently undamage structure. Hence the safe use of composite structure requires an understanding of the progression of damage because of multi-impacts. Although the impact strength under single-impact loading is widely studied, the problem of composites under repeated impacts has attracted less attention [72]. In this section, the present analysis model was used to study the multi-impacts problem of stiffened composite laminated plate, and the damage accumulation problem of the multi-impacts was also investigated. In the analysis process of the multi-impacts, all of the parameters for each impact kept unchanged except the material properties which would be affected by the damage accumulation.

Impact responses of concentrically stiffened composite laminated plates subjected to multi-impacts are shown in Fig. 25. In this numerical example, the thickness of stiffeners is 7.0 mm and the radius of impactor is 6.0 mm. The impact velocity of the first and second impacts is 24.7487 m/s, and the total impact energy of two impacts equals to that results from one impact with initial velocity 35 m/s. In the first loading–unloading cycle, the loading speed of contact force of the 1st impact is larger than that of the 2nd impact, while the maximum contact force of the 2nd impact is larger than that of the 1st impact. The reason is that the damages induced by the 1st impact significantly reduce the stiffness near the contact region. In the second loading–unloading cycle, the peak values of contact force of the 1st and 2nd impact are roughly equal. Although the start time of loading and unloading of the 1st impact is earlier that of the 2nd impact, the end time of the whole impact process of 1st and 2nd impact is the same. For the single impact at the initial velocity 35 m/s, the percentages of the residual velocity in the initial velocity are 43.6474% (residual velocity 15.2766 m/s). For the multi-impact at the initial velocity 24.7487 m/s (first impact) and 24.7487 m/s (second impact), the percentages of the residual velocity in the initial velocity are 41.9060% (residual velocity 10.3712 m/s) and 43.1178% (residual velocity 10.6711 m/s), respectively. The central deflection of laminated plate and displacement of impactor of the 2nd impact are larger than those of the 1st impact because of the stiffness reduction near the contact region resulted from damage accumulation of the 1st impact.

Damage variations distributions of concentrically stiffened laminated plate subjected to multi-impacts (1st and 2nd impact) are shown in Fig. 26. It can be seen from Fig. 26 that compared with the damages induced by 1st impact the range of damages have been broadened by the 2nd impact even though the damages arised due to 1st or 2nd impact are limited. Composite structures are prone to sudden failure under the action of repeated small energy impacts, and what's even worse, the extension and cumulative process is not detectable from visible observation. Therefore, the dangers of repeated small energy impact for composite structures are greater than the dangers of single larger energy impact.

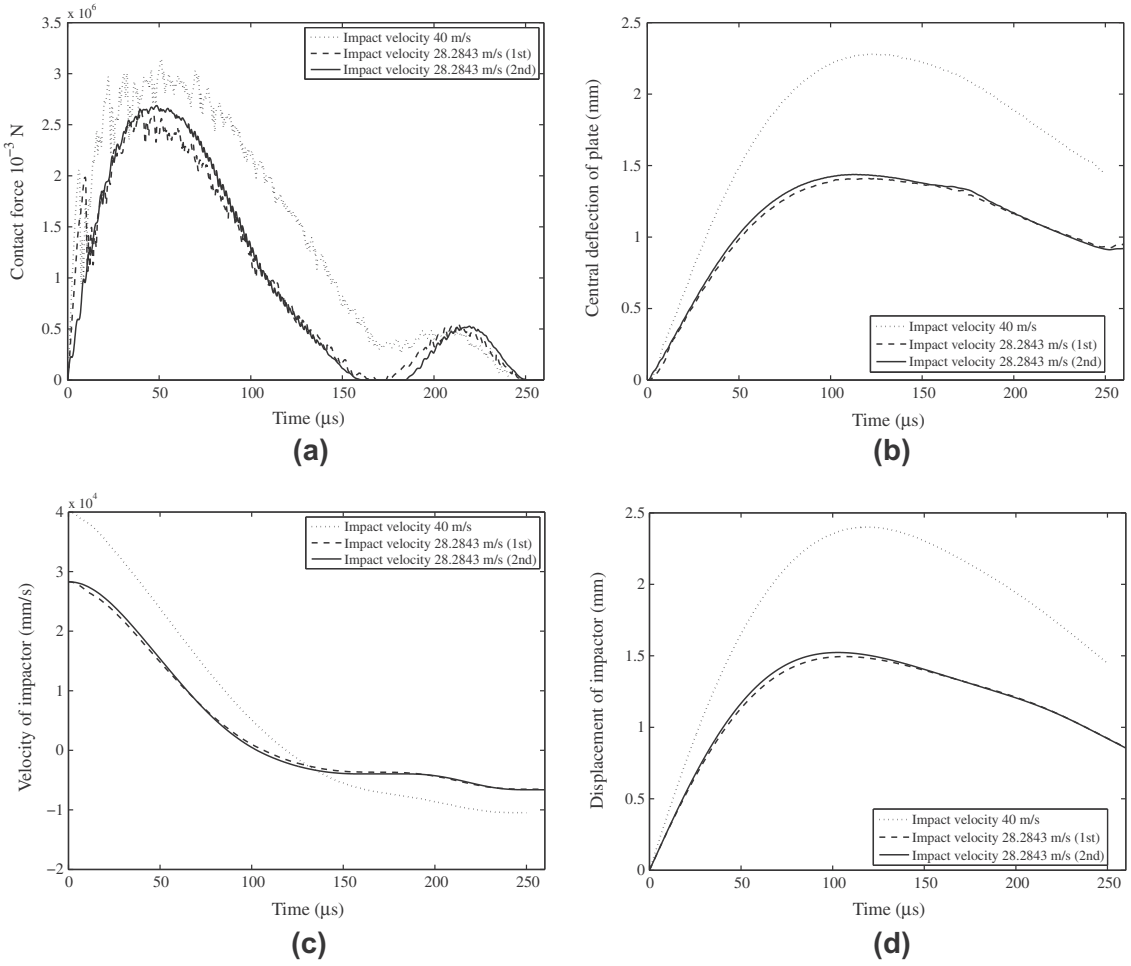

Fig. 27. Impact responses of parallelly stiffened composite laminated plates subjected to multi-impacts. (a) Contact force; (b) displacement w of plates in contact point, (c) velocity of impactor and (d) displacement of impactor.

Compared with the damage induced by the single impact with initial velocity 35 m/s (see Fig. 13), the damage accumulations induced by the multi-impacts (1st and 2nd impact) are significantly smaller than those resulted from the single impact, though the sum of impact energy of the multi-impacts is equal to the impact energy of the single impact (see Fig. 27).

Impact responses of parallelly stiffened composite laminated plates subjected to multi-impacts are shown in Fig. 25. And the damage variations distributions of parallelly stiffened laminated plate subjected to multi-impacts (1st and 2nd impact) are shown in Fig. 28. In this numerical example, the thickness of stiffeners is 7.0 mm and the radius of impactor is 6.0 mm. The impact velocity of the first and second impacts is 28.2843 m/s, and the total impact energy of two impacts equal to that results from one impact with initial velocity 40 m/s. For the single impact at the initial velocity 40 m/s, the percentages of the residual velocity in the initial velocity are 26.19% (residual velocity 10.4770 m/s). For the multi-impact at the initial velocity 28.2843 m/s (first impact) and 28.2843 m/s (second impact), the percentages of the residual velocity in the initial velocity are 23.0969% (residual velocity 6.5328 m/s) and 23.4218% (residual velocity 6.6247 m/s), respectively.

It can be seen from Figs. 25 and 28 that the multi-impacts behavior of parallelly stiffened composite laminated plates is similar to that of concentrically stiffened laminated plates. The loading speed of contact force of the 1st impact is larger than that of the 2nd impact in the first loading–unloading cycle, and the peak values of contact force of the 1st and 2nd impact are roughly equal in the second loading–unloading cycle. The difference is that the maximum contact force of the 2nd impact is slightly larger than that of the 1st impact.

6. Concluding remarks

In the present work, a LW/SE method, modified nonlinear Hertz's law and the progressive failure model are combined to develop a method for low impact responses and impact-induced damages analysis of the composite stiffened plates. In this analysis model, the transient response analysis model of the stiffened composite laminated plate is estiblished by using the LW/SE method and Newmark method, the contact force between the stiffened plate and impactor is obtained by the modified nonlinear Hertz's law with Newmark method, and the predicition of impact-induced damages is carried out with the progressive failure model. Without any assumption about the stiffeners, the accurate stress and strain responses can be obtained by using the present low-impact analysis method for the composite laminated plates with arbitrarily complex stiffeners. As a result of the adoption of the progressive failure model in this method, the accumulation and extension of the impact-induced damages can be predicted accurately as well.

Several numerical examples are carried out to study the influence of parameters on the impact response and impact-induced

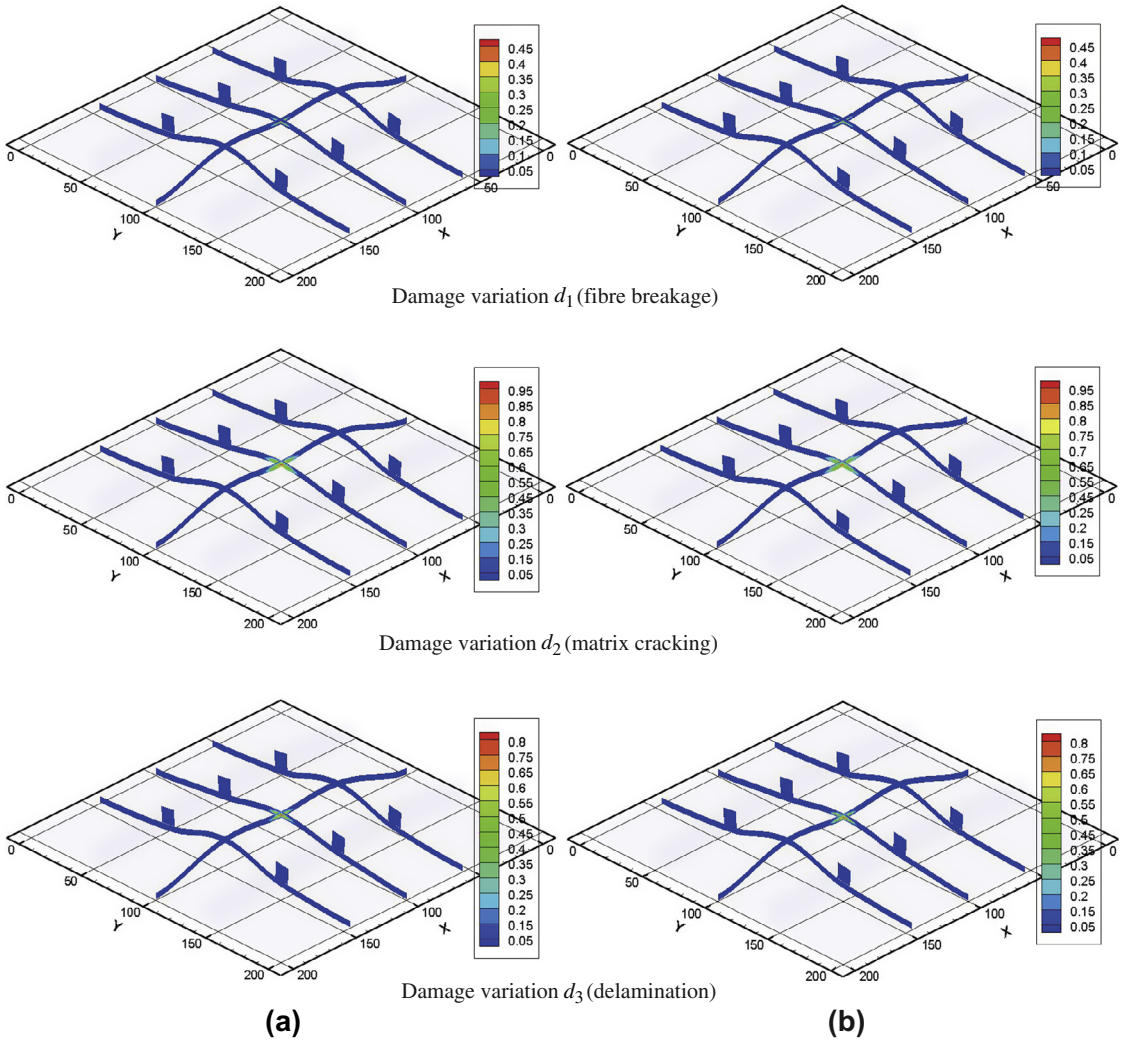

Fig. 28. Damage variations distributions of parallelly stiffened laminated plate subjected to multi-impacts. (a) First impact; and (b) second impact.

damage is investigated, such as the impact velocity, radius of impactor and thickness of stiffeners. In addition, the present analysis model is used to study the multi-impacts problem of stiffened composite laminated plate. Based on results obtained under various cases, observations have been summarized in respective section. These observations lead to certain broad conclusions which are stated as:

1. For the stiffened composite laminated plate, the stresses and strains of the laminated plate and stiffeners can be calculated accurately by using the present impact analysis method, and the impact-induced damages also can be precisely predicted. Furthermore, the present model can be used to obtain the low-impact responses and impact-induced damages of the composite laminated plate stiffened with complex stiffeners without any assumption and simplification.
2. The load point in thickness direction has no effect on the impact responses except the maximum contact force of the secondary impact if the impact-induced damage is not token into account, while with the progressive damage model the load point in thickness direction has significant influences on the impact responses. In order to obtain a reasonable impact response, the equivalent point load resulted from impact should be acted on the middle surface of laminated pates.
3. For the stiffened composite laminated plates subjected to low-impact, the fiber breakage and delamination of laminated plate is generally very limited and confined to the region near the contact area between the impactor and the laminates. With the impact energy increasing, the matrix cracking is extending constantly far away from the contact area. And the matrix cracking and delamination are the main part of the impact-induced damages for the stiffened composite laminated plates subjected to low-impact.
4. For the concentrically stiffened composite laminated plates subjected to low velocity impact, there are three danger zones: the contact region, the middle region of the stiffeners along the direction with weaker stiffness and the interface region between the laminated plate and stiffeners along the direction with stronger stiffness. For the parallelly stiffened composite laminated plates subjected to low velocity impact, there are two danger zones: the contact region between impactor and laminated plate and the interface region between the laminated plate and stiffeners along the direction with stronger stiffness. The deflection of the stiffened composite laminted plate decreased with the increasing of the stiffness of the stiffeners, while the impact-induced damages just the opposite. Therefore, the impact resistant ability and the stiffness of the stiffened composite laminated plate are contradictory.

5. Composite structures are prone to sudden failure under the action of repeated small energy impacts, and what's even worse, the extension and cumulative process are not detectable from visible observation. Therefore, the danger of repeated small energy impact for composite structures is greater than the danger of single larger energy impact.

Acknowledgements

Supported by the National Basic Research Program of China (2010CB832701), National Natural Science Foundation of China (11272180) and Tsinghua University Initiative Scientific Research Program.

References

[1] Li D, Qing G, Liu Y. A layerwise/solid-element method for the composite stiffened laminated cylindrical shell structures. Compos Struct 2013;98:215–27.
[2] Li D, Liu Y, Zhang X. A layerwise/solid-element method of the linear static and free vibration analysis for the composite sandwich plates. Compos Part B: Eng 2013;52:187–98.
[3] Abrate S. Impact on laminated composite materials. Appl Mech Rev 1991;44(4):155–90.
[4] Abrate S. Impact on laminated composites: recent advances. Appl Mech Rev 1994;47:517.
[5] Abrate S. Modeling of impacts on composite structures. Compos Struct 2001;51(2):129–38.
[6] Sun C, Chattopadhyay S. Dynamic response of anisotropic laminated plates under initial stress due to impact of a mass. J Appl Mech 1975;43:693–8.
[7] Dobyns A. Analysis of simply-supported orthotropic plates subject to static and dynamic loads. AIAA J 1981;19(5):642–50.
[8] Whitney J, Pagano N. Shear deformation in heterogeneous anisotropic plates. Tech. rep., DTIC Document; 1970.
[9] Sun C, Chen J. On the impact of initially stressed composite laminates. J Compos Mater 1985;19:490–504.
[10] Cairns D, Lagace P. Transient response of graphite/epoxy and kevlar/epoxy laminated subjected to impact. AIAA J 1989;27(11):1590–6.
[11] Wu H, Chang F. Transient dynamic analysis of laminated composite plates subjected to transverse impact. Comput Struct 1989;31:453–66.
[12] Gong S, Toh S, Shim V. The elastic response of orthotropic laminated cylindrical shells to low-velocity impact. Compos Eng 1994;4:247–66.
[13] Gong S, Toh S, Shim V. Impact response of laminated shells with orthogonal curvatures. Compos Eng 1995;5:257–75.
[14] Nosier A, Kapania R, Reddy J. Low-velocity impact of laminated composite using a layerwise theory. Comput Mech 1994;13:360–79.
[15] Chandrashekhara K, Schroeder T. Nonlinear impact analysis of laminated cylindrical and doubly curved shells. J Compos Mater 1995;29:2160–79.
[16] Choi IH, Lim CH. Low-velocity impact analysis of composite laminates using linearized contact law. Compos Struct 2004;66(1):125–32.
[17] Choi HY, Wu H-YT, Chang F-K. A new approach toward understanding damage mechanisms and mechanics of laminated composites due to low-velocity impact: Part 2 – Analysis. J Compos Mater 1991;25(8):1012–38.
[18] Choi HY, Downs R, Chang F-K. A new approach toward understanding damage mechanisms and mechanics of laminated composites due to low-velocity impact: Part 1 – Experiments. J Compos Mater 1991;25(8):992–1011.
[19] Choi H, Chang F. A model for predicting damage in graphite/epoxy laminated composites resulting from low-velocity point impact. J Compos Mater 1992;26(14):2134–69.
[20] Kim SJ, Goo NS, Kim TW. The effect of curvature on the dynamic response and impact-induced damage in composite laminates. Compos Sci Technol 1997;57(7):763–73.
[21] Krishnamurthy K, Mahajan P, Mittal R. A parametric study of the impact response and damage of laminated cylindrical composite shells. Compos Sci Technol 2001;61(12):1655–69. http://dx.doi.org/10.1016/S0266-353(01)00015-X. <http://www.sciencedirect.com/science/article/pii/S026635380100015X>.
[22] Krishnamurthy K, Mahajan P, Mittal R. Impact response and damage in laminated composite cylindrical shells. Compos Struct 2003;59(1):15–36. http://dx.doi.org/10.1016/S0263-822(02)00238-6. <http://www.sciencedirect.com/science/article/pii/S0263822302002386>.
[23] Gong S, Lam K. Transient response of stiffened composite plates subjected to low velocity impact. Compos Part B: Eng 1999;30(5):473–84.
[24] Seydel R, Chang FK. Impact identification of stiffened composite panels: 2. Implementation studies. Smart Mater Struct 2001;10(2):370.
[25] Seydel R, Chang FK. Impact identification of stiffened composite panels: 1. System development. Smart Mater Struct 2001;10(2):354.
[26] Faggiani A, Falzon B. Predicting low-velocity impact damage on a stiffened composite panel. Compos Part A: Appl Sci Manuf 2010;41(6):737–49.
[27] Kukreti AR, Rajapaksa Y. Analysis procedure for ribbed and grid plate systems used for bridge decks. J Struct Eng 1990;116(2):372–91.
[28] Kukreti A, Cheraghi E. Analysis procedure for stiffened plate systems using an energy approach. Comput Struct 1993;46(4):649–57.
[29] Brubak L, Hellesland J, Steen E. Semi-analytical buckling strength analysis of plates with arbitrary stiffener arrangements. J Construct Steel Res 2007;63(4):532–43.
[30] Mukhopadhyay M. Stiffened plates in bending. Comput Struct 1994;50(4):541–8.
[31] Siddiqi ZA, Kukreti AR. Analysis of eccentrically stiffened plates with mixed boundary conditions using differential quadrature method. Appl Math Modell 1998;22(4):251–75.
[32] Mukhopadhyay M, Mukherjee A. Finite element buckling analysis of stiffened plates. Comput Struct 1990;34(6):795–803.
[33] Deb A, Booton M. Finite element models for stiffened plates under transverse loading. Comput Struct 1988;28(3):361–72.
[34] Palani G, Iyer N, Rao T. An efficient finite element model for static and vibration analysis of eccentrically stiffened plates/shells. Comput Struct 1992;43(4):651–61.
[35] Li D, Liu Y. Three-dimensional semi-analytical model for the static response and sensitivity analysis of the composite stiffened laminated plate with interfacial imperfections. Compos Struct 2012;94(6):1943–58.
[36] Qing G, Qiu J, Liu Y. Free vibration analysis of stiffened laminated plates. Int J Solids Struct 2006;43(6):1357–71.
[37] Pengcheng S, Dade H, Zongmu W. Static, vibration and stability analysis of stiffened plates using b spline functions. Comput Struct 1987;27(1):73–8.
[38] Rossow M, Ibrahimkhail A. Constraint method analysis of stiffened plates. Comput Struct 1978;8(1):51–60.
[39] Sheikh A, Mukhopadhyay M. Analysis of stiffened plate with arbitrary planform by the general spline finite strip method. Comput Struct 1992;42(1):53–67.
[40] Biswal K, Ghosh A. Finite element analysis for stiffened laminated plates using higher order shear deformation theory. Comput Struct 1994;53(1):161–71.
[41] Carrera E, Zappino E, Petrolo M. Analysis of thin-walled structures with longitudinal and transversal stiffeners. J Appl Mech 2012;1:335.
[42] Carrera E, Zappino E, Filippi M. Free vibration analysis of thin-walled cylinders reinforced with longitudinal and transversal stiffeners. J Vib Acoust 2013;135:011019.
[43] Sadek EA, Tawfik SA. A finite element model for the analysis of stiffened laminated plates. Comput Struct 2000;75(4):369–83.
[44] Guo YL, Lindner J. Analysis of elastic-plastic interaction buckling of stiffened panels by spline finite strip method. Comput Struct 1993;46(3):529–36.
[45] Peng L, Kitipornchai S, Liew K. Analysis of rectangular stiffened plates under uniform lateral load based on fsdt and element-free galerkin method. Int J Mech Sci 2005;47(2):251–76.
[46] Peng L, Liew K, Kitipornchai S. Buckling and free vibration analyses of stiffened plates using the fsdt mesh-free method. J Sound Vib 2006;289(3):421–49.
[47] Sapountzakis E, Katsikadelis J. Analysis of plates reinforced with beams. Comput Mech 2000;26(1):66–74.
[48] Tanaka M, Matsumoto T, Oida S. A boundary element method applied to the elastostatic bending problem of beam-stiffened plates. Eng Anal Bound Elem 2000;24(10):751–8.
[49] Wen P, Aliabadi M, Young A. Boundary element analysis of shear deformable stiffened plates. Eng Anal Bound Elem 2002;26(6):511–20.
[50] de Oliveira Neto L, de Paiva JB. A special bem for elastostatic analysis of building floor slabs on columns. Comput Struct 2003;81(6):359–72.
[51] Nairn J, Hu S. Matrix microcracking. Compos Mater Ser 1994. 187–187.
[52] Yang S, Sun C. Indentation law for composite laminates. ASTM STP 1982;787:425–49.
[53] Yang HT, Saigal S, Masud A, Kapania R. A survey of recent shell finite elements. Int J Numer Methods Eng 2000;47(1–3):101–27.
[54] Reddy J. A general non-linear third-order theory of plates with moderate thickness. Int J Non-Linear Mech 1990;25(6):677–86.
[55] Whitney J. The effect of transverse shear deformation on the bending of laminated plates. J Compos Mater 1969;3(3):534–47.
[56] Reissner E. Note on the effect of transverse shear deformation in laminated anisotropic plates. Comput Methods Appl Mech Eng 1979;20(2):203–9.
[57] Carrera E. Evaluation of layerwise mixed theories for laminated plates analysis. AIAA J 1998;36(5):830–9.
[58] Carrera E. Developments, ideas and evaluations based upon reissner's mixed variational theorem in modeling of multilayered plates and shells. Appl Mech Rev 2001;54(4):301–29.
[59] Reddy J. Mechanics of laminated composite plates and shells: theory and analysis. 2nd ed. CRC press; 2003.
[60] Carrera E. Theories and finite elements for multilayered plates and shells: a unified compact formulation with numerical assessment and benchmarking. Arch Comput Methods Eng 2003;10(3):215–96.
[61] Cinefra M, Belouettar S, Soave M, Carrera E. Variable kinematic models applied to free-vibration analysis of functionally graded material shells. Eur J Mech – A/Solids 2010;29(6):1078–87.
[62] Ferreira A, Carrera E, Cinefra M, Roque C. Analysis of laminated doubly-curved shells by a layerwise theory and radial basis functions collocation, accounting for through-the-thickness deformations. Comput Mech 2011;48(1):13–25.
[63] Hashin Z, Rotem A. A fatigue failure criterion for fiber reinforced materials. J Compos Mater 1973;7(4):448–64.
[64] Hashin Z. Analysis of composite materials. J Appl Mech 1983;50(2):481–505.
[65] Murray Y, Schwer L. Implementation and verification of fiber-composite damage models; 1990.

[66] Sleight DW. Progressive failure analysis methodology for laminated composite structures. Citeseer; 1999.
[67] Bazant Z, Oh B. Crack band theory for fracture of concrete. Mater Struct 1983;16:155–77.
[68] Maimi P, Camanho P, Mayugo J, Davila C. A continuum damage model for composite laminates: Part 2 – Computational implementation and validation. Mech Mater 2007;39:909–19.
[69] Lapczyk I, Hurtado J. Progressive damage modeling in fiber-reinforced materials. Compos Part A: Appl Sci Manuf 2007;38:2333–41.
[70] Wu H. Impact damage of composite. Ph.D. thesis, Stanford University; 1986.
[71] Wang Y, Tong M, Zhu S. Three-dimensional nonlinear progressive damage analysis on composite laminates based on continuum damage mechanics. J Nanjing Univ Aeronaut Astronaut 2009;41(6):709–14.
[72] Amaro A, Reis P, de Moura M, Neto M. Influence of multi-impacts on gfrp composites laminates. Compos Part B: Eng 2013.